Taras Shevchenko National University of Kyiv
Astronomical Observatory

Astronomy and Space Physics

Book of Abstracts

International Conference

October 18 – October 21, 2022

Kyiv, Ukraine

Scientific organizing committee (SOC)

Chair Vasyl' Ivchenko (Ukraine)
Co-chair: Volodymyr Efimenko (Ukraine)

Conference Secretary I. Lyk'yanyk (Ukraine)

SOC Members
Artem Bohdan (Germany), Bohdan Hnatyk (Ukraine), Olexandra Ivanova (Slovakia), Liliya Kazantseva (Ukraine), Vsevolod Lozitsky (Ukraine), Gennadi Milinevsky (Ukraine), Sergiy Parnovsky (Ukraine), Oleh Petruk (Italy), Vira Rosenbush (Ukraine), Sergiy Silich (Mexico), Valentyna Zharkova (UK), Valery Zhdanov (Ukraine), Yaroslav Yatskiv (Ukraine), Vasyl' Yurchyshyn (USA).

Local organizing committee (LOC)

Chair: Vasyl' Ponomarenko (Ukraine)
Secretary: Alena Mozgova (Ukraine)

LOC Members
Asen Grytsai, Liliya Kazantseva, Ivan Yakovkin

E-mail: aoconf@ukr.net

Place of the meeting
Astronomical observatory of the Taras Shevchenko national university of Kyiv, Observatorna str., 3

CONTENTS

ПЛЕНАРНІ ЗАСІДАННЯ

PLENARY SESSIONS

Planetary and astrophysical high Mach-number shocks: kinetic simulations vs in-situ measurements

A. Bohdan[1]

[1]Deutsches Elektronen-Synchrotron DESY, Zeuthen, Germany

High-Mach-number collisionless shocks are found in planetary systems and supernova remnants (SNRs). Electrons are heated at these shocks to temperatures well above the Rankine–Hugoniot prediction. However, the processes responsible for causing the electron heating are still not well understood. We use a set of large-scale particle-in-cell simulations of nonrelativistic shocks in the high-Mach-number regime to clarify the electron heating processes. The physical behaviour of these shocks is defined by ion reflection at the shock ramp. Further interactions between the reflected ions and the upstream plasma excite electrostatic Buneman and two-stream ion–ion Weibel instabilities. Electrons are heated via shock surfing acceleration, the shock potential, magnetic reconnection, stochastic Fermi scattering, and shock compression. The main contributor is the shock potential. The magnetic field lines become tangled due to the Weibel instability, which allows for parallel electron heating by the shock potential. The constrained model of electron heating predicts an ion-to-electron temperature ratio within observed values at SNR shocks and in Saturn's bow shock. We also present evidence for field amplification by the Weibel instability. The normalized magnetic field strength strongly correlates with the Alfvenic Mach number, as is in-situ observed at Saturn's bow shock.

Effects of the Tonga volcano explosion on January 15, 2022

L.F. Chernogor

V.N. Karazin Kharkiv National University, Kharkiv, Ukraine

The eruption of the Hunga-Tonga-Hunga-Ha'apai volcano on January 15, 2022 was the largest recorded since the eruption of Krakatoa in 1883. The parameters of its explosion are comparable to the parameters of the explosions of a number of large volcanoes. Five explosions of the underwater Tonga volcano (20.54°S, 175.38°W) took place over the 04:00–05:02 UT period. The most powerful explosion of the volcano with an ~ 4–5-km-wide caldera and a crater of ~ 20–30-m diameter occurred at about 04:15 UT, which acted to trigger an earthquake of magnitude 5.8. The eruption lasted for 12 ± 2 h during which 2.9 Gt of rock occupying 1.9 km^3 volume was thrown out. The mean mass flow rate is estimated to be 67 kt/s, and a mean volumetric discharge rate to be 4.4×10^4 m^3/s. The plume from this explosion reached a peak height of 58 km into the mesosphere at a mean speed of 33 m/s. The mass of sulphur dioxide ejected by the explosion was estimated to attain a value of 4×10^8 kg, while the mass of sulphuric acid to be 8×10^8 kg. The atmospheric plume from the volcanic eruption was carried out by the wind over a distance of 15 Mm at an average horizontal speed of 20 m/s.

Volcanic flow. The hot tephra of an ~10-m initial radius rose with an ~ 100–250 m/s initial speed and had almost the same speed on emerging out of the water. The vertical movement of the flow in the conducting sea water acted to produce the local magnetic effect of ~ 140–630 nT. In the air, the volcanic flow increased its radius to ~ 400 m and attained an altitude of less than 2 km. Further, the rise of hot explosion products (plume) occurred due to convection. To estimate the height of the plume rise, the following relationship was obtained.

Tsunami. The volcano's explosion produced two types of tsunami. The first moved with the speed of 200 m/s where 4 km is the mean depth of the ocean. The second type of tsunami was due to the movement of a ground-coupled air wave and moved with the speed of 315 m/s. The tsunami height attained 15 m off the shores of the Kingdom of Tonga, up to 3 m near Chili, up to 2 m near Peru, up to 1 m off the shores of the U.S.A., and 0.1–0.3 m in the Atlantic Ocean and the Mediterranean Sea.

Atmospheric waves. The volcanic explosion acted to excite waves of various kinds in the atmosphere. Near the source, the shock wave developed traveling with a speed of greater than 1 km/s. Further away propagated sound, infrasound, and the Lamb wave with the speed of 315 m/s. The Lamb wave traveling virtually without attenuation propagated five times around the globe, while the echoes of the explosion were heard in Alaska (distance is 9 Mm). The wave had a cylindrical wave front.

Explosive wave energy. Different authors have estimated the energy of the explosive wave to be 4–330 Mt TNT. Our estimates made using the amplitude of the explosive wave registered by the worldwide infrasound network of the International Monitoring System for the verification of the Comprehensive Nuclear-Test-Ban Treaty in the 64–823 km range and taking into account the cylindrical wave front of the Lamb wave have yielded 31 ± 4 Mt TNT, and the durations of the compression and rarefaction phases were estimated to be about 20 min.

Conclusion. A comprehensive analysis and modeling have been carried out of the physical processes in the ocean, the atmosphere, the ionosphere, and the magnetosphere, which accompanied the Tonga volcanic eruption. Quasi-sinusoidal and aperiodic perturbations have been revealed in all components of the Earth–atmosphere–ionosphere–magnetosphere (EAIM) system, and their mechanisms have been analyzed. The energetics of waves of various kinds and of the perturbations in the geophysical fields has turned out to be sufficient to maintain the long-term and global restructuring of coupling between the subsystems in the EAIM system.

Measurements of the CNO solar neutrino flux by Borexino

V.V. Kobychev[1] (on behalf of the Borexino Collaboration)

[1]Institute for Nuclear Research of NAS Ukraine, Kyiv, Ukraine

The CNO (Carbon-Nitrogen-Oxygen) cycle of hydrogen fusion is the sub-dominant source of solar energy, with two orders of magnitude lower rate than the dominant proton-proton cycle. However, the CNO cycle is dominant in the main sequence stars heavier than the Sun and is thus the main energy source of net stellar luminosity in the present-time Universe. The only way of direct observation of the CNO cycle is detection of neutrinos which are produced in the different branches of the cycle with the total rate of two emitted electron neutrino per one created ^{4}He nucleus. Detection of the CNO solar neutrino provides direct information on the metallicity of the solar core, i.e. on the abundance of the elements heavier than helium, including C, N, and O, which catalyses the hydrogen burning in the CNO cycle.

Borexino was the 280-ton liquid scintillation detector with an unprecedented radiopurity that allowed to prove the existing of CNO neutrinos for the first time. It was placed at the Laboratori Nazionali del Gran Sasso (LNGS), Italy, and was taking data from May 2007 to October 2021. The null hypothesis (absence of CNO neutrinos) is excluded with about 7σ significance by the analysis of the compete Phase III dataset of Borexino. The measured fluxes of CNO neutrinos agrees very well with the class of so-called “high-metallicity” Standard Solar Models (SSM) and is in a moderate tension with the predictions of the “low-metallicity” SSMs.

Electron energization through stochastic shock drift acceleration at low Mach number shocks in galaxy clusters

O. Kobzar[1], J. Niemiec[2], T. Amano[3], M. Hoshino[3], S. Matsukiyo[4], Y. Matsumoto[5], M. Pohl[6,7]

[1]Faculty of Materials Engineering and Physics, Cracow University of Technology, Kraków, Poland
[2]Institute of Nuclear Physics PAS, Kraków, Poland
[3]Department of Earth and Planetary Science, University of Tokyo, Tokyo, Japan
[4]Faculty of Engineering Sciences, Kyushu University, Fukuoka, Japan
[5]Department of Physics, Chiba University, Chiba, Japan
[6]Institute of Physics and Astronomy, University of Potsdam, Potsdam-Golm, Germany
[7]DESY, Zeuthen, Germany

Shock waves in cosmic plasma are generally considered as appropriate places of the particle acceleration. They can be found in a number of astrophysical objects at different scales e.g. Earth's bow shock, solar flares, supernova remnant (SNR) shocks, and large-scale shocks in clusters of galaxies. Radio and X-ray observations of radio relics indicate that electrons are accelerated to relativistic nonthermal energies at merger shocks in galaxy clusters. These large-scale shocks can also be sites of ultra-high-energy cosmic ray production.

It is assumed that diffusive shock acceleration (DSA) produces synchrotron-radiating electrons but the process of electron pre-acceleration from thermal to supra-thermal energies is poorly known yet. Particularly, in the case of galaxy clusters, merger shocks are found to propagate with low Mach numbers ($M << 10$) in hot plasmas with $\beta >> 1$. Recent studies with 1D and 2D Particle-In-Cell (PIC) simulations have showed the important role of the shock drift acceleration (SDA) and scattering processes for the electron energization at such conditions.

Using large-scale fully-kinetic two-dimensional particle-in-cell (PIC) simulations of a quasi-perpendicular subluminal shock with low sonic Mach number ($M_s = 3$) and propagating in hot intracluster medium with plasma beta $\beta = 5$, we have recently demonstrated that the main electron pre-acceleration mechanism is stochastic shock-drift acceleration (SSDA). In this process electrons are confined at the shock by pitch-angle scattering off

turbulence and gain energy while drifting along the motional electric field. We showed that multi-scale magnetic turbulence, including ion-scale shock rippling modes, is essential for electron energization. This turbulence is driven by effective ion and electron temperature anisotropies in the entire shock transition. Wide-energy non-thermal electron distributions are formed both upstream and downstream of the shock and the maximum energy of the electrons is sufficient for their injection into DSA. Here we report on our new PIC simulation studies of SSDA process in a range of shock obliquity angles. We show that SSDA persists in facilitating the electron injection in rippled shocks.

Primordial black holes as dark matter

A. Kusenko[1,2]

[1]Department of Physics and Astronomy, University of California Los Angeles, Los Angeles, USA
[2]Kavli Institute for the Physics and Mathematics of the Universe, Tokyo, Japan

A number of different cosmological scenarios can lead to production of primordial black holes (PBHs) in amounts sufficient to account for all or part of dark matter. I will review theoretical understanding, astrophysical manifestations, and ongoing search for primordial black holes.

Non-transient gamma-ray binaries: current status and perspectives

D. Malyshev[1]

[1]Institut für Astronomie und Astrophysik Tübingen,
Eberhard Karls Universität Tübingen, Tübingen, Germany

Gamma-ray binaries are a subclass of high-mass binary systems whose energy spectrum peaks at high energies (E > 100 MeV) and extends to very high energies (E > 100 GeV) gamma-rays. In this review talk I summarize properties of well-studied non-transient gamma-ray binaries (like e.g. PSR B1259-63 and LS I +61 303) as well as briefly discuss poorly known systems (e.g. HESS J1832-093 or 4FGL J1405.1-6119). I discuss the recent advances of theoretical modelling and successes of VHE instruments in observations of these peculiar systems.

Cosmological magnetic fields

A. Neronov[1,2]

[1]Université de Paris, Astroparticle and Cosmology Laboratory,
Paris, France
[2]EPFL Lausanne, Switzerland

I will review current knowledge of intergalactic magnetic field and argue that such a field of cosmological origin may be populating voids of the Large Scale Structure. I will then discuss perspectives of deteciton of such field with the Cherenkov Telescope Array.

Globally averaged signals in 21 cm line of atomic hydrogen from Dark Ages, Cosmic Dawn and Reionization

B. Novosyadlyj[1,2], Yu. Kulinich[1], V. Shulga[2,3]

[1]Ivan Franko National University of Lviv, Lviv, Ukraine,
[2]Jilin University, Changchun, P.R. China,
[3]Institute of Radio Astronomy of NASU, Kharkiv, Ukraine

We analyze formation of the redshifted hyperfine structure line 21 cm of hydrogen atom in the cosmological epochs Dark Ages ($20<z>200$), Cosmic Dawn ($10<z<20$) and Reionization ($6<z<10$). In order to study its sensitivity to the values of cosmological parameters, and physical conditions and composition of intergalactic medium, the evolution of the globally averaged differential brightness temperature in the line was calculated in various cosmological models. Variations of the depth of the Dark Ages absorption line at z_{max}~80 (ν~18 MHz) with variations of the cosmological parameters Ω_b, Ω_{cdm}, Ω_Λ, Ω_K and H_0 in the ΛCDM model are illustrated. The model with post-Planck parameters predicts a value of the differential brightness temperature in the center of the absorption line ~30-40 mK. It is also shown that the position and depth of the Cosmic Dawn absorption line at $10<z<20$ ($60<\nu<130$ MHz), due to the Wouthuysen-Field effect, is mainly determined by the spectral energy distribution of the first sources of light (or model of the first light). If reionization occurs at $z_{ri}=7\pm1$ (Planck Collaboration 2020, Bouwens et al. 2015, ApJ, 811, 140; Banados et al. 2018, Nature, 553, 473; Davies et al. 2018, ApJ, 864, 142) , then the differential brightness temperature in the center of this absorption line is ~10-50 mK. During the reionization at $7<z<10$ ($130< \nu <180$ MHz), the emission with an amplitude of ~5 mK is possible. It is also shown that the temperature, density, and degree of ionization of the baryonic component are decisive in calculating the intensity of the 21 cm absorption/emission line from the these epochs. The predictions of the standard ΛCDM model agree with the observed data of the SARAS 3 telescope (Singh et al. 2022).

Space missions Kepler and TESS: new horizons of modern astrophysics

Ya. Pavlenko[1]

[1]Main Astronomical Observatory, National Academy of Sciences of Ukraine, Kyiv, Ukraine

Some results of the Kepler and TESS space missions data analysis are discussed. These data provide a good opportunity to get new knowledge about our stars and planetary systems, their evolution as well as to get better understanding of our own planetary system.

Magnetic field throughout the supernova remnant evolution

O. Petruk[1,2], V. Beshley[2], T. Kuzyo[2]

[1]INAF-Palermo Astronomical Observatory, Palermo, Italy
[2]Institute for Applied Problems in Mechanics and Mathematics, Lviv, Ukraine

Magnetic field is an important component in many astrophysical systems. It manifests itself through a number of multimessenger channels, one of the most known is the radio emission. We review the role and behaviour of magnetic field on different stages of supernova remnant evolution as well as show how the polarization observations may be used to determine the initial structure of magnetic field in the circumstellar meduim before a supernova event.

On highly relativistic gravitodynamics

R.M. Plyatsko[1], M.T. Fenyk[1]

[1]Pidstryhach Institute for Applied Problems in Mechanics and Mathematics, Lviv, Ukraine

An effective approach for description of the physical properties of the gravitational field in general relativity was proposed by K. Thorne and J. Hartle (Phys. Rev. D 31, 1815, 1985). For this purpose the components of Riemann's tensor in the local tetrad coordinates are considered. Among these components, the two important types are determined: gravitoelectric and gravitomagnetic. The first of them reflects the properties of the gravitational field similar in a certain sense to the properties of the electric field. Accordingly, the second type has a clear analogy with the magnetic field in classical electrodynamics. At the same time, the gravitoelectric components determine the effect of tidal forces, while the gravitomagnetic components are manifested in the spin-gravity coupling. We consider spin-gravity effects from the point of view of an observer moving relative to a Schwarzschild gravitational field source with an arbitrary velocity. An important point is that the values of the components of the gravitomagnetic field depend significantly on the velocity of the observer: they are proportional to the relativistic Lorentz factor or to the second power of this factor. As a result, according to the Mathisson-Papapetrou (MP) equations, which describe motion of a spinning test particle in gravitational field, just these components deviate its motion from geodesic in Schwarzschild's metric from the point of view of the commoving observer. Different examples of action of the highly relativistic spin-gravity coupling on the particle's motion are considered. We use the adequate supplementary condition for the MP equations that was introduced by Mathisson (1937). An alternative condition proposed by Tulczyjew (1959s) is satisfactory when the particle's velocity is not very high and, in general, cannot be used at high velocities. For example, under this condition a spinning particle, which begins motion in Schwarzschild's field with the velocity less than the speed of light, can be accelerated to the superluminal velocity. Another unphysical result under this condition follows from analysis of the expression for the spinning particle 4-momentum through its 4-velocity: it is shown that for the highly relativistic tangential velocity the values of the momentum components become imaginary.

Globular cluster multiple population problem and the molecular gas properties in star-forming regions with a suppressed gas outflow.

S. Silich[1]

[1]Instituto Nacional de Astrof´isica, Óptica y Electrónica, Puebla, Mexico

Globular clusters are not simple stellar populations. They contain at least two stellar generations: one similar to the host galaxy field stars and another one that requires the primordial gas to be polluted with high temperature hydrogen-burning products. In extremely compact and dense star-forming clouds a global star cluster wind could be suppressed. In this case the stellar feedback is unable to expel the leftover gas from the cluster. Massive stars remain embedded into a dense residual gas and stir it moving in the gravitational well of the system. Here the molecular gas properties in such young stellar clusters are discussed. It is assumed that the cloud collapse terminates and the star formation ceases when a balance between the turbulent pressure and gravity and between the turbulent energy dissipation and regeneration rates is established. These two conditions result in an equation that determines the residual gas density distribution that, in turn, allows one to determine the leftover gas other characteristics, estimate the star formation efficiency and propose a scenario for the multiple population formation.

Half a century of AGN photometry and where it has taken us

H. Winkler[1]

[1]Department of Physics, University of Johannesburg, South Africa

Fifty years ago Ukrainian astronomy played a leading part in some of the earliest photometric studies of active galactic nuclei (AGN) and their variations. This method of investigation is finally unravelling some of the structure, mechanisms and physical properties of these enigmatic objects. Previously elusive periodic variations are now being identified in isolated objects, while reverberation mapping is gradually allowing the determination of black hole masses for an increasing number of AGN.

This talk will focus on results obtained with the flux variation gradient analytical technique. The earliest application thereof included data collected at the Crimean Observatory in the 1970's. It has since developed into a powerful tool to perform host galaxy-nucleus separation and to quantify nuclear obscuration.

New UBVu′g′r′ photometric data of AGN will be presented that has been obtained with the Las Cumbres Observatory global robotic telescope network in the last two years. In addition to improved nuclear obscuration and luminosity estimates, the preliminary analysis of the results explores possible differences in the intrinsic flux distribution and the degree of variability between several AGN sub-classes. It also examines suspected deviations from the Milky Way reddening law in the interstellar material in some of the inclined AGN host galaxies.

Erupting Solar Magnetic Flux Ropes and the Bz Challenge: Understanding Details of CME Propagation in the Interplanetary Media

V.B. Yurchyshyn

Big Bear Solar Observatory, New Jersey Institute of Technology, USA

Understanding the connection between magnetic topologies of a coronal mass ejection (CME) as observed closer to the Sun and in the interplanetary medium close to the Earth is vital for successful predictions of geomagnetic storms. Recent solar and magnetospheric data convincingly demonstrate that fast CME originating from near the solar disk center are the major cause of extreme space weather events. Moreover, topology and helicity of the ejected fields tends to be mainly preserved as the ejecta propagates and evolves in the interplanetary space. The interplanetary CME that is often observed near the Earth as a well organized helical structure called a magnetic cloud (MC) is the result of expansion of the original ejecta and its interaction with the heliospheric plasma and magnetic fields that may cause the ejecta to alter its shape, rotate and shed its magnetic flux. Therefore the probability of a strong geomagnetic storm to occur as well as its intensity depend on both initial properties of the erupted structure and the further interactions that the ejecta may be subjected to as it expands into the heliosphere. Detailed understanding of this interaction may shed light on the problems related to connecting solar surface phenomena to their interplanetary counterparts. In this talk I will briefly review current progress on the CME evolution in the heliosphere.

Mysteries of particle acceleration and propagation in flaring atmospheres

Valentina Zharkova

Northumbria University, Newcastle on Tyne, UK

In this talk I will explore using the 3D Particle-In-Cell (PIC) approach particle acceleration in reconnecting current sheets with and without magnetic islands, explore pure particle effects and formation of kinetic turbulence induced by accelerated particle. I will also demonstrate a self-consistent formation of top-loop and footprint sources of HXR and MW emission in reconnecting magnetic loops of solar flares. It will be shown ith time-dependent Fokker-Planck approach that particle transport from the top to footprints and back to the top iis governed by the electric circuits of accelerated particles (direct and returning electrons). The FP solutions show that accelerated particle precipitation leads to formation important observational effects of HXR and MW emission and polarisation reported in solar flares. Furthermore, using joint solutions of the FP and weve equation, it is shown that electric circuits of direct and returning electrons produce substantial plasma turbulence at lower atmospheric levels. The interaction of accelerated particles with this turbulence is shown to lead to electron beam pinching and formation of radio bursts of the third types with zebra patterns.

АСТРОФІЗИКА, ГРАВІТАЦІЯ І КОСМОЛОГІЯ

ASTROPARTICLE PHYSICS, GRAVITATION AND COSMOLOGY

On the electromagnetic radiation reaction in de Sitter space

A.A. Duviryak[1], Yu.G. Yaremko[1]

[1]Institute for Condensed Matter Physics of NAS of Ukraine, Lviv, Ukraine

We discuss a radiation reaction force acting on a point charged particle in de Sitter space (dS). To derive the radiation reaction force one utilizes an electromegnetic Green's function (EGF) and a regularization procedure. Both are defined ambiguously. We examine different EGFs in dS and apply different regularizations. First, we apply the Gobbs construction of EGF to the conformally flat metrics of de Sitter space and arrive at the minimal covariant generalization of the Abraham-Lorentz radiation reaction force. On the other hand, the substitution of EGF proposed by Narlikar into the DeWitt-Brheme-Gobbs equations yields an additional non-local "tail" term. The discrepancy is resolved by manifestation that Narlikar's function actually is not EGF in dS. In order to reduce the source of ambiguities, we apply the requirement of invariance with respect to the group of isometry of dS. Starting with de Sitter invariant EGF found by Higuchi and Cheong, we develop the de Sitter invariant regularization procedure and apply it to the formally divergent Lorentz force which backreacts on the charge. This self-force contains both divergent and finite terms, and the latter are responsible for the radiation reaction. Alternatively, we insert the expressions for the field strengths in Noether quantities corresponding to de Sitter group. We decompose these quantities into bound (divergent) and radiative (finite) parts. The divergent terms are absorbed by kinematic particle's characteristics within the renormalization procedure. Radiative terms together with already renormalized particle's individual characteristics constitute the total conserved quantities of closed particle plus field system. Their differential consequences yield the effective equations of motion of radiating charge in an external electromagnetic field which reproduce the DeWitt-Brheme-Gobbs equations with zero "tail" term.

Non-thermal radiation from galaxy clusters

R. Hnatyk[1], V. Voitsekhovskyi[1]

[1]Astronomical Observatory of Taras Shevchenko National University of Kyiv, Kyiv, Ukraine

Galaxy clusters (GCs) are the largest and most massive gravitationally bounded objects in the large-scale structure of the Universe. Due to high (of the order of a few keV) temperature of virialized gas in the intracluster medium (ICM) and the presence of cosmic rays (CRs), GCs are effective sources of thermal X-ray and non-thermal lepton (synchrotron) radiation. GCs are also store rooms for the CRs because the time of CR diffusive escape from GCs exceeds the age of the Universe. However, non-thermal hadronic gamma-ray emission (mainly due to proton-proton collisions of CRs and thermal ICM and subsequent neutral pions' decay) from GCs has not yet been robastly detected. In this paper, we model the expected nonthermal hadronic gamma-ray and neutrino fluxes from Coma cluster and Hercules cluster and evaluate the prospects for registration of this radiation by existing (Fermi-LAT, LHASSO, IceCube) and planned ground-based (CTA, IceCube-Gen2) detectors.

Milky Way globular clusters subsystem in cosmological timescale. Interaction with the Galactic center

M.V. Ishchenko[1,2], M.O. Sobolenko[1], P.P. Berczik[3,4,1,2], O.O. Sobodar[1]

[1]Main Astronomical Observatory, National Academy of Sciences of Ukraine, Kyiv, Ukraine
[2]Fesenkov Astrophysical Institute, Almaty, Kazakhstan
[3]Astronomisches Rechen-Institut, Zentrum für Astronomie, University of Heidelberg, Heidelberg, Germany
[4]Konkoly Observatory, Research Centre for Astronomy and Earth Sciences, Eötvös Loránd Research Network (ELKH), MTA Centre of Excellence, Budapest, Hungary

The main idea of the work is to carry out the dynamic evolution of the orbits of Globular Cluster subsystems sample lookback time up to 10 Gyr. This allows us to estimate the possibility of GCs interaction with the Galactic center that dynamically changed in the past. To reproduce the structure of the Galaxy in time, we used five external potentials, which were selected from the large-scale cosmological database IllustrisTNG-100, and which in their characteristics (mass and size of disk and halo) are similar to the physical values of the Milky Way at the present day. In these potentials, we reproduced the orbits of 147 GCs in 10 Gyr lookback time using our own high-order N-body parallel dynamic code phi-GPU code. For each of the GCs was generated additional 1000 initial data with randomized initial radii velocities within the observation data errors: proper motions and radial velocity (with normal distribution). To identify clusters that have interaction with the Galactic center, we used the criteria of relative distance: it must be less than 100 pc. Applying these simple criteria, we obtained statistically significant rates of close passages of the GCs with each other and with the Galactic center.

Formations and radio emission of the first molecules of the Dark Ages

Yu. Kulinich[1], B. Novosyadlyj[1,2], V. Shulga[2,3]

[1]Ivan Franko National University of Lviv, Lviv, Ukraine,
[2]Jilin University, Changchun, P.R. China,
[3]Institute of Radio Astronomy of NASU, Kharkiv, Ukraine

The signal from the first molecules formed in the Dark Ages was evaluated. For this, the kinetics of the formation of the first H_2, HD and HeH^+ molecules in the Dark Ages, the population of their rovibrational levels, and the luminescence/absorption of the first molecules against the cosmic microwave background radiation caused by collisional de-/excitations of their rovibrational levels were calculated. It was concluded that, within the framework of the standard cosmological model, the presence of first molecules leads to the partial absorption of quanta of the cosmic microwave background, distorting its spectrum. The amplitude of such a distortion, however, is very small - three orders of magnitude less than the projected sensitivity limit of "Voyage-2050" aimed at measuring distortions in the CMB spectrum. The probable presence of the primordial magnetic field will lead to the radio emission of the first molecules with an amplitude attainable for registration in the planned missions of measuring distortions in the CMB spectrum.

The early evolution of supernova remnants shaped by the supernova ejecta structure

T. Kuzyo[1], O. Petruk[1,2]

[1]Institute for Applied Problems in Mechanics and Mathematics, Lviv, Ukraine
[2]INAF-Palermo Astronomical Observatory, Palermo, Italy

A supernova remnant on its early stages of evolution is characterized as ejecta-driven which means that the supernova ejecta is playing the key role both in dynamics of the forward shock wave and post-shock characteristics of the supernova remnant. We study the effect of the initial 3D structure of the supernova ejecta on details of the resulting post-shock structures in a supernova remnant. For this purpose we perform a series of 3D MHD simulations of supernova remnant evolution with varying initial ejecta distributions and interstellar number densities.

Results of optical photometric research of AGN Markarian 421 and ES 1426+428

V.O. Ponomarenko[1], A.O. Simon[1,2], V.V. Vasylenko[2], I.O. Izviekova[3]

[1]Taras Shevchenko National University of Kyiv, Kyiv, Ukraine
[2]National Center Junior academy of sciences of Ukraine, Kyiv, Ukraine
[3]Main Astronomical Observatory of NAS of Ukraine, Kyiv, Ukraine

Results of systematical monitoring of AGN Markarian 421 and ES 1426+428 are presented. The observations were obtained during 2018-2020 using the telescope AZT-8 (D = 70 cm, F = 2.8 m) of the observation station Lisnyky of Astronomical Observatory of Taras Shevchenko National University of Kyiv. The AZT-8 is equipped with broadband Johnson/Bessel UBVRI filters and the PL4710-1-BB-E2V CCD (1027x1048 pixels, 13x13 μm/pixel, the scale is 0.95 "/pixel, the field of view is 16.2 angular minutes).

The fluxes of energy from the objects of research have been turned into visible stellar magnitudes with the help of standard stars. Light curves for objects ES 1426+428 and Markarian 421 were plotted. We determined the amplitude of variability of brightness for Short-term variability and Long-term variability for object ES 1426+428. The variability of color indexes for ES 1426+428 was also investigated. For AGN Markarian 421 the Intraday variability was determined. The search for mechanisms of brightness change and the search for correlations between the optical and gamma ranges were also carried out.

Dark matter profiles of SPARC galaxies

A. Rudakovskyi[1]

[1]Bogolyubov Institute for Theoretical Physics, Kyiv, Ukraine

Stellar and gas kinematics of galaxies are a sensitive probe of the dark matter distribution in the halo. The popular fuzzy dark matter models predict the peculiar shape of density distribution in galaxies: specific dense core with sharp transition to the halo. Moreover, fuzzy dark matter predicts scaling relations between the dark matter particle mass and density parameters. In this work, we use a Bayesian framework, Modified Newtonian Dynamics and several dark matter halo models to analyse the stellar kinematics of galaxies using *the Spitzer Photometry & Accurate Rotation Curves* database. We then employ a Bayesian model comparison to select the best halo density model. We find that more than half of the galaxies prefer the fuzzy dark model against standard dark matter profiles (NFW, Burkert, and cored NFW). While this seems like a success for fuzzy dark matter, we also find that there is no single value for the particle mass that provides a good fit for all galaxies.

Inflation or dark matter from *f*(*R*) gravity

Yu.V. Shtanov[1,2]

[1]Bogolyubov Institute for Theoretical Physics, Kyiv, Ukraine
[2]Astronomical Observatory of Taras Shevchenko National University of Kyiv, Kyiv, Ukraine

A large class of metric $f(R)$ gravity theories translate into scalar-field (scalaron) models with hilltop or tabletop potentials in the Einstein frame. Inflationary evolution in hilltop/tabletop models can proceed in two alternative directions: towards the stable point at small R describing the observable universe, or towards the asymptotic region at large R. Inflationary evolution towards the stable point in models with extended tabletop potentials agrees very well with CMB observations and requires scalaron mass $m \approx 3 \times 10^{12}$ GeV. In $f(R)$ models, gravity can become asymptotically free, with $G_{\mathrm{eff}} \to 0$, at infinite or large finite values of the scalar curvature R. A universe evolving towards this asymptotically free gravity region will either run into a "Big-Rip" singularity, or inflate eternally.

Metric $f(R)$ gravity theory can alternatively describe dark matter if its scalaron mass m lies in the rrange 4 meV $\leq m \leq$ 1.2 MeV. In this case, there arise limitations on the inflationary energy scale for the Hubble parameter $H_{\mathrm{inf}} < 10^5$–10^7 GeV, or for reheating temperature $T_{\mathrm{r}} < 10^{11}$–10^{12} GeV.

Statistics of light curves of gravitationally microlensed oblate sources

V.M. Sliusar[1], V.I. Zhdanov[2]

[1] Department of Astronomy, University of Geneva, Switzerland
[2] Astronomical observatory of Taras Shevchenko National University of Kyiv, Kyiv, Ukraine.

Microlensing of a remote source by stars of the foreground galaxy is considered with a focus on the statistical effects due to the source oblateness. We build the amplifications curves (related with the light curves), which describe the dependence of the source brightness enhancement when it moves through the caustic field on the source plane. With this aim we derive the field of amplification coefficients for the set of pointlike masses; their random positions in each were distributed homogeneously inside a circle, which was big enough to avoid boundary effects. The amplification map has been derived by the ray shooting method using the hierarchical tree algorythm. This procedure has been repeated for a number of random tests. For each realization of the microlensing field the convolution of the amplification map with the initial brightness distribution over the source yields the amplification curve for every time moment. We show that there is a significant difference of the autocorrelation function for this curves between sources with different ellipticity. However, practical usage of the results is complicated be the necessity of a continuous monitoring.

Circular orbits of test particles interacting with gravitational and scalar fields described by the Fisher solution

O. S. Stashko[1,2,3,4], V. I. Zhdanov[1]
[1] Astronomical observatory of Taras Shevchenko National University of Kyiv, Kyiv, Ukraine
[2] Frankfurt Institute for Advanced Studies, Frankfurt am Main, Germany
[3] Goethe Universität, Frankfurt am Main, Germany
[4] CERN, Theoretical Physics Department, Geneva, Switzerland

The test particle motion around the static spherically symmetric configuration represented by the well-known Fisher solution of General Relativity in presence of a massless linear scalar field (SF) is investigated. Besides the purely gravitational interaction, we introduce a direct interaction of the particles with SF in the form of the power-law and exponential couplings in the particle action. The resulting equations are used to study stable and unstable circular orbits (CO) around the configuration. The focus is on the non-connected distributions of the stable CO, when different regions of the latter are separated either by rings of the unstable CO, or domains when there are no circular orbits at all. We show that the coupling essentially affects the qualitative properties of the stable CO distributions; there are some new topological features, which are absent for the geodetic motion in the case of the Fisher metric.

Cosmic-ray ensembles simulations: a new method, status and perspectives

O. Sushchov[1] (for the CREDO Collaboration)

[1]Institute of Nuclear Physics Polish Academy of Sciences, Krakow, Poland

Cosmic rays undergo numerous interactions with matter, fields and background radiation while propagating in space. As a result, particle cascades of various shapes, constituents and spatial extent are generated. Potential registration of at least parts of such phenomena, referred to as cosmic-ray ensembles (CRE), at Earth would open a new channel of

cosmic-ray astrophysics. CRE-dedicated research is one of the main objectives of the Cosmic-Ray Extremely Distributed Observatory (CREDO) Collaboration scientific program. In the talk we highlight one of the most important aspects of the relevant study, the simulation of CRE formation and behavior. We present a new method of CRE simulation and illustrate its use focusing at the synchrotron radiation by high energy electrons as the leading process of particle cascading. Preliminary results as well as perspectives of the research are discussed.

An approach to decoupling of the Maxwell equations in the case of null field

Y.V. Taistra[1], V.O. Pelykh[1], A.M. Kuz[1]

[1]Pidstryhach Institute for Applied Problems in Mechanics and Mathematics, Lviv, Ukraine

Astrophysical objects, such as black holes, neutron stars etc. generate strong gravitational fields, and the general relativity theory must be used to describe electromagnetic field propagation in their vicinity. The Maxwell equations in the pseudo-Riemannian space of general relativity are a strongly coupled system of the first-order PDEs. Decoupling methods for a such system were developed by Teukolsky (1973), Cohen, Kegeles (1974, 1979), and Stewart (1979). Maxwell equations in the Teukolsky approach decouple in the Petrov type D space-times. Electromagnetic equations for Herz potential decouple in generalized Goldberg-Sachs space-times, assuming the additional condition of algebraical specialty to Herz spinor (null one-way Herz field). An approach to decoupling Maxwell equations in Kasner space-time was developed by Bochner (2021).

We assume that the Maxwell field is null, which means that both electromagnetic invariants are equal to zero (pure electromagnetic waves). Under this assumption, the system of Maxwell equations decouple. Two of the four decoupled equations are the first-order quasilinear PDEs. We consider decoupled equations in the Kerr space-time and apply Teukolsky form of solution (Teukolsky ansatz). This enables a more simple (2-dimensional) decoupled system, which is promising from a computational point of view.

Optical emission lines in X-ray galaxies on z<0.35

A. Tugay[2], N. Pulatova[1,4], L. Zadorozhna[2,3]

[1]Max Planck Institute for AstronomyGernamy.
[2]Taras Shevchenko National University of Kyiv, Physical faculty, Kyiv, Ukraine
[3]Faculty of Physics, Astronomy and Applied Computer Science, Jagiellonian University, Poland
[4]Main Astronomical Observatory of National Academy of Science of Ukraine, Kyiv, Ukraine

X-ray band is consequential to study active processes in galaxies such as star formation and nuclear activity. In our work, we present a new sample of 1347 galaxies with X-ray emission at z<0.35. The sample was compiled by cross-correlation of the Sloan Digital Sky Survey (SDSS) catalog of galaxies with emission lines and XMM-Newton database 4XMM DR10 which contains up to million sources in the 0.2-12 keV range. The redshift restriction follows the fact that for more distant galaxies H alpha line is out of SDSS spectral sensitivity. The principle of including galaxy to sample was a maximal value of separation between X-ray and optical center of 6 arcseconds. SDSS spectra of our galaxies contain optical lines H beta, [OIII] 5007, [OI] 6300, [NII] 6548, [NII] 6584, [SII] 6717 and [SII] 6731. These lines are widely used for AGN classifications with Baldwin-Philip-Terlevich (BPT) diagrams since 1981. Kewley (2006) used an empirical relation between line intensities to distinguish LINERS and Seyferts on BPT diagram. Torbaniuk (2021) used this relation for the sample of X-ray-selected SDSS galaxies, but used only one line from [NII] and [SII] doublets. We insist on considering both doublet lines for active galaxy classification and plan to build an improved BPT diagram for X-ray SDSS galaxies with our sample. We also considered distributions of coordinates, redshifts, and fluxes of our galaxies. The new sample will be used for deep studies of optical emission in X-ray galaxies to understand the origin of X-ray emission of galaxies. We also plan to determine the excitation of optical emission in X-ray galaxies.

Unveiling the nature of the unidentified gamma-ray sources in the sky region of the magnetar SGR 1900+14

V. Voitsekhovskyi[1], B. Hnatyk[1], R. Hnatyk[1], V. Zhdanov[1]

[1]Astronomical Observatory of Taras Shevchenko National University of Kyiv, Kyiv, Ukraine

Supernova remnants (SNRs), star formation regions (SFRs), and pulsar wind nebulae (PWNe) are prime candidates for Galactic PeVatrons. The non-thermal high-energy (HE, $\varepsilon > 100$ MeV) and very high-energy (VHE, $\varepsilon > 100$ GeV) γ-ray emission from these sources should be a promising manifestation of acceleration processes. We investigate the possibility to explain the HE and VHE γ-ray emission from the sky region of the magnetar SGR 1900+14 as a signature of cosmic rays accelerated in above-mentioned sources. To this end, we simulate the γ-ray emission from the extended Fermi-LAT HE source 4FGL J1908.6+0915e, the extended VHE H.E.S.S. source candidate HOTS J1907+091, and the point-like HAWC TeV source 3HWC J1907+085, which are spatially coincident with the SNR G42.8+0.6, the magnetar SGR 1900+14, and the star-forming region W49A. The simulations are performed within the hadronic and leptonic models. We show that the observed γ-ray emission from the region of the magnetar SGR 1900+14 can, in principle, include contributions of different intensities from all three types of (potentially confused) sources. The considered in detail cases of a magnetar-connected but still undetected SNR and a PWN are the most promising ones, but with a serious requirement on the energy reserve of radiated CR particles –of the order of 10^{51} d^2_{10kpc} erg for sources at a distance of d ∼10 kpc. Such energy reserve can be provided by the magnetar-related Hypernova and/or magnetar wind nebula remnant created by the newborn millisecond magnetar with the large supply of rotational energy E_{rot} ∼10^{52} erg.

АСТРОМЕТРІЯ І МАЛІ ТІЛА СОНЯЧНОЇ СИСТЕМИ

ASTROMETRY AND SMALL BODIES OF THE SOLAR SYSTEM

Photometric results of (52768) 1998 OR2 and (99942) Apophis

M. Husárik[1], O. Ivanova[1, 2, 3]

[1]Astronomical Institute of the Slovak Academy of Sciences, Slovakia
[2]Main Astronomical Observatory of the National Academy of Sciences of Ukraine, Ukraine
[3]Taras Shevchenko National University of Kyiv, Astronomical Observatory, Ukraine

We report an analysis of photometric observations for two potentially hazardous asteroids – (52768) 1998 OR2 and (99942) Apophis. Data for 1998 OR2 was obtained in March – April 2020 and for Apophis in February – March 2021, when both objects experienced their close approaches to Earth.

The observations of both PHAs were carried out with the 0.61-m *f*/4.3 Newton reflector at the Skalnaté Pleso Observatory (Slovakia, IAU code 056) and CCD camera SBIG ST-10XME. We obtained photometric data using broad-band Johnson-Cousins *B*, *V*, and *R* filters, 2×2 binning, and a resolution of 1.07 arcsec/px. The calibration with dark and flatfield frames was applied and we used a differential aperture photometry technique to obtain light curves.

Asteroid 1998 OR2 was observed for 9 nights. From each night we obtained 3 – 4 hr series in BVR filters, from which we determined the exact synodic rotation periods about at 4.11 hours. Data from the *V* filter we used to determine the absolute magnitude *H*, which has a value of 15.72 ± 0.02 mag. We kept the slope parameter *G* at 0.15 because of the narrow range of phase angles. Next, we calculated the approximate effective diameters of the asteroid using an albedo value of 0.2. These varied only minimally between 2.1 and 2.3 km on each observing night, with a mean value of 2.14 ± 0.06 km. Color photometry also allowed us to determine an approximate taxonomic class in the Tholen classification. With high probability, the asteroid's surface is dominated by a metallic material, which characterizes the X-class. Our finding is confirmed by Hromakina et al. (2021).

In the spring of 2021, perhaps the most famous asteroid, Apophis, approached the Earth. We used this time to obtain photometric material to refine the physical characteristics known so far. The aim was not to make long-term observations to determine the rotational period, as this is known, a fact complicated by the excited rotational state (tumbling). We focused on

finding the *B-V* and *V-R* color indices, the absolute magnitude, and the diameter. After the first observations, it was clear that either the shape of the object is highly elongated or the rotation is not performed along one axis. The values of the effective diameter varied significantly from 0.31 to 0.40 km each night. We observed a similar effect when determining the absolute magnitude, which we calculated to be 19.08 ± 0.06 mag (with fixed G = 0.24). Similarly to the previous asteroid, we used color photometry. It shows almost unequivocally that Apophis is classified as an S-type asteroid. A similar finding was obtained by Hromakina et al. (2021) and Lin et al. (2018).

The motion of dust particles ejected from the surface of asteroid 6478 Gault

V. Reshetnyk[1,2], O. Ivanova[1,2,3]

[1] National Taras Schevchenko University of Kyiv, Ukraine
[2] Main astronomical observatory of National academy of sciences of Ukraine, Ukraine
[3] Astronomical Institute of Slovak Academy of Science, Slovakia

Some asteroids demonstrate not comet-like dust activity. The reasons for the ejection of dust particles from the surface of asteroids are not always obvious. Simulations show that these could be electrostatic forces, centrifugal forces, collisions with meteoroids, etc. Important factors in the dynamics of dust are the radiation pressure, possibly the interplanetary magnetic field and the solar wind too. In our work we simulated the motion of dust particles of various sizes. The source of activity was a centrifugal force. The parameters of asteroid Gault were taken as input data for the simulation. Different modes of activity were considered: point and extended active region. Optical parameters were calculated for each test particle. The solar radiation pressure was calculated based on the actual position of the asteroid Gault at a given moment. Synthetic photometric images of the tail were constructed based on the obtained trajectories of the dust particles. The simulation was carried out for different values of the orientation of the axis of rotation and the period of the asteroid's rotation.

Modified geometrical model of cometary jets

V.V. Kleshchonok

Astronomical observatory of Taras Shevchenko National University of Kyiv, Ukraine

The simple geometric model of the jet was developed to interpret the pattern of jets. It has simple set of parameters: the period of rotation of the comet nucleus, the coordinates of the north pole, the speed of departure of the jet particles. Additionally, the model uses the location of the Sun, the Earth, and the comet. In the geometric model, it is assumed that the emission of matter occurs at a constant speed. Emissions of dust particles occur only when the active area is illuminated by the Sun. It allows to quickly calculate the structure of jets, look at the dynamics of formation and evolution of appearance. We can select possible parameters of visible structures, see dynamics of formation of jets in the coma of a comet. The found model parameters can be used as an initial approximation for other, more complex models. The geometric model has been successfully used to interpret the structural features of the coma for a number of comets. It made it possible to obtain the orientation of the axis of rotation of the nucleus of a number of comets, the periods of rotation, to estimate the velocity of matter in the jets, and the position of active sites on the comet's nucleus.

The modified geometric model has a number of improvements and is a further development of the simple geometric model. A number of additional parameters have been introduced. The possible thermal inertia of the core was taken into account, which manifests itself in a delay in the start of the outflow of matter with the rising of the Sun over the active region and its completion after sunset. The possible deviation of the substance ejection direction from the radial direction is also taken into account. An important feature of the modified geometric model is the ability to take into account the width of the jets. An original approach was used for this, which makes it possible to determine the boundaries of the jet for any orientation in space. These improvements make it possible to more accurately determine the parameters of rotation of the comet nucleus in complex cases.

Investigations of comet C/2014 B1 (Schwartz)

I. Luk'yanyk[1], O. Ivanova[1,2,3], V. Rosenbush[1], V. Kleshchonok[1], L. Kolokolova[4]

[1] Astronomical Observatory of Taras Shevchenko National University of Kyiv, Ukraine
[2] Astronomical Institute of the Slovak Academy of Sciences, Slovakia
[3] Main astronomical observatory of National academy of sciences of Ukraine, Ukraine
[4] University of Maryland, USA

We present results of the comprehensive optical observations of the unique disk-like comet C/2014 B1 (Schwartz) with perihelion distance 9.56 au. Quasi-simultaneous long-slit spectra, as well as photometric and polarimetric images with g-sdss and r-sdss filters, were obtained with the 6-m telescope of the Special *Astrophysical* Observatory on 2017 January 23. The BVR photometric observations of the comet were also obtained at the 2-m telescope of the Peak Terskol Observatory (North Caucasus) on 2017 January 31. We did not reveal any molecular emissions in the spectra. Two nearly linear jets oriented along the *position angles* of 179°± 1° and 350°± 1° were detected in the coma. Our data demonstrate that the observed disk-like shape of the coma and position of jets remained unchanged, despite the changing observational geometry, for more than 4 years. The most realistic model for explanation of such stable orientation of jets is the existence two active sources located near the north and south poles of the *rotating* nucleus whose diameter was determined being between 7.6 and 12.2 km depending on the albedo, 0.1 and 0.04, respectively. High activity of the comet is characterized by the high dust production $Af\rho$ which significantly varied, from 4440 to 3357 cm between 2017 January 23 and 31. A significant difference between the radial surface brightness profiles of jets and the ambient (undisturbed by the jets) coma is found. The color of the cometary dust is redder than that of the Sun: on January 23, $V-R = 0.58^{m} \pm 0.05^{m}$, and on January 31, $B-V = 0.85^{m} \pm 0.05^{m}$ and $V-R = 0.54^{m} \pm 0.05^{m}$. The color of the jet structures is much redder than of the ambient coma. Very red color of the nucleus ($V-R = 0.93^{m} \pm 0.19^{m}$) was derived. There are spatial variations of the color and polarization over the coma. The near-nucleus coma is characterized by a low negative degree of polarization (−1% at the phase angle 2.1°) and red color (up to $\sim 0.7^{m}$),

while at the periphery, at about 100 000 km, there is a high negative polarization (–6.5%) and a bluer color (0.6^m – 0.45^m). Our modeling showed that the observed trends in color and polarization, as well as the brightness profiles, can be explained by fragmentation of aggregated particles, formed by CO_2/H_2O ices, silicates and organics, which are of radius ~ 1 mm near the nucleus and ~ 10 micron at the periphery.

Features of fireball phenomena observations in the daytime

A.V. Golubaev[1], A.M. Mozgova[2]

[1]Institute of Astronomy, V.N. Karazin KhNU, Kharkiv, Ukraine
[2]Astronomical Observatory of Taras Shevchenko KNU, Kyiv, Ukraine

This paper presents an overview of some greatest fireball phenomena that were observed during the daytime:

- A small asteroid 2008 TC3 Almahata Sitta impact on the Earth's surface in the form of meteorite fragments on October 7, 2008 at 05:46 AM local time (UT+3);
- Chelyabinsk meteorite fall on February 15, 2013 at 09:20 AM local time (UT+06);
- Ozerki meteorite fall on June 21, 2018 at 04:16 AM local time (01:16 UT);
- Novo Mesto meteorite fall on February 28, 2020 at 10:31 AM local time (9:31 UT).

We present the methods for positional and photometric measurements of fireball phenomena which are observed in the daytime, a technique for determining the kinematic characteristics (velocity, parameters of the atmospheric trajectory, etc.) and calculating the elements of the heliocentric orbits of meteoroids.

Problems of using geocentric and geodetic coordinate systems for processing of double-station meteor observations

P. M. Kozak

Taras Shevchenko National University of Kyiv, Kyiv, Ukraine

Methods of processing of double-station meteor observations include the use of local coordinate systems related to observational points, being brought later to a common coordinate system. Then, the results of previous geometric data processing have to be transformed into geocentric coordinate system for the future calculation of heliocentric velocity of a meteoroid and its orbital elements. The classic approach was in using topocentric horizontal coordinate systems. Nevertheless, it seems to be much easier to use an approach proposed in [1], where the base is the geocentric coordinate system (Z axis is directed to the world pole, X axis corresponds to Greenwich meridian, Y axis orientation is aimed to complete the right-oriented three vectors) and its topocentric analogues whose datum points corresponds to the observational points. Such an approach is justified by the fact that the spherical coordinates of the meteor image dots, which are the input parameters for the triangulation processing, are calculated in equatorial coordinate system, and the given system is connected just with the geocentric one only by a rotation angle around Z axis, which is nothing else but the sidereal time.

However, at the cataloging of meteor kinematic parameters such data as, for instance, its altitude above sea level H, or geographic latitude φ have to belong to geodetic (geographic) coordinate system, but the computations are made in geocentric one. The question arises: how important is the transformation of given parameters from one coordinate system to another, and what error appears if do not realize such a transformation. We have to note, that in opposite to the altitude above sea level H the latitude (longitude is not changed at the transformation) of projection of a dot on a meteor trail onto the earth surface is basically a number not using anywhere later. But there is an exclusive situation when the bright bolide flights (as a rule relatively slow), and who finally can fall onto earth surface as a meteorite, and must be found – for this reason the projection of the meteor train onto earth surface has to be determined with maximum precision.

In the given work we analyze the problem of transformation of meteor geocentric coordinates into its geodetic (geographic) coordinates for

"meteor altitudes" from zero to 80-130 km, and according to the latest investigations – up to 200 km, for any latitudes of observations. The difference in geocentric and geodetic altitudes of a meteor for different latitudes is considered; and it is shown that the given difference may be neglected with the precision of a meter for any latitude. However, the difference in latitudes is important, and its maximum corresponds to latitude near 45° and is 0.19° (which corresponds to 22 km on earth surface), decreasing to zero for $\varphi = 0°$ and $\varphi = 90°$. The view of dependence for "geodetic minus geocentric" latitude $\Delta\varphi$ for the given altitude H is very close to the function $A \cdot \cos(2\pi\varphi - \pi/2)$, but such a dependence is conditioned by low earth eccentricity – the function becomes asymmetric for bigger value of it. The results of fitting given function are presented, the coefficient of the model are calculated with Monte-Carlo method what save computation time significantly.

Modernization of astronomical complex of observational station Lisnyky

M.I. Buromsky[1], V. L. Karbovsky[2], V.V. Kleshchonok[1], M. V. Lashko[2]

[1]Astronomical observatory of Taras Shevchenko National University of Kyiv, Ukraine
[2]Main Astronomical Observatory of the National Academy of Sciences of Ukraine

The Lisnyky observation station (international code 585) is actively used for observations of small bodies and for educational purpose. The station operates two telescopes AZT-8 (D=700 mm, F=2830 mm, D/F=1:4) and AZT-14 (D=480 mm, F=7715 mm, D/F=1:16). They have an outdated design and need to be modernized to meet the modern requirements of observational astronomy. The world practice of modernizing optical telescopes is reduced, as a rule, to installing new modern light receivers, changing the optical system, improving optical characteristics by aluminizing mirrors. Light receivers are now CCD image sensors, the use of which allows you to significantly increase the penetrating power (to observe fainter objects) and the temporal and spatial resolution of telescopes. Modern light receivers are equipped with automatic filter units with various sets of astronomical filters. Different sets of light receivers are used for different tasks of observational astronomy. The concept of modernization of

the observation complex based on the AZT-14 and AZT-8 telescopes was developed according to these modern requirements.

A new Moravian C4-16000ES CCD camera (4096 × 4096 pixels, 9 × 9 μm) with a UBVRI light filter unit of the Johnson-Cousins photometric system was installed at the main focus of the AZT-8 telescope in 2021. In this version, the telescope is used to monitor small bodies and search for new comets and asteroids, photometric and positional observations of comets, observations of active galactic nuclei.

An optical reducer (4.5 times) with a block of broadband light filters BVRI light filters was developed and manufactured for the AZT-14 telescope in order to increase the field of view on the CCD array, reduce the size of star images and increase the light power of the telescope. A new block of 8 comet narrowband filters, which is used with the Apogee Alta U47 CCD camera, was designed and manufactured for observations of comets. An electronic control system, which includes the following main electronic components: a light filter position sensor board, an electronic board, a stable frequency generator, a stepper motor driver, a controller for controlling all electronic components and for communication with a personal computer, was developed and manufactured for control the unit.

Dynamics of the CO+ coma of comet 29P/Schwasmann–Wachmann: the global MHD ENLIL Solar Wind Prediction model results

O. Agapitov[1,2], O. Ivanova[1,3,4], D. Odstrci[l,5,6]

[1]Taras Shevchenko National University of Kyiv,
[2]Space Sciences Laboratory, University of California Berkeley,
[3]Astronomical Institute of the Slovak Academy of Sciences,
[4]Main Astronomical Observatory of the National Academy of Sciences of Ukraine
[5]George Mason University, USA
[6]NASA/GSFC, USA

Comet-centaur 29P/Schwassmann–Wachmann 1 was observed in CO+ emission and continuum during 2007–2009 using the 6-m Big Telescope Alt-azimuth at the Special Astrophysical Observatory of the Russian Academy of Sciences [1]. We analyzed the morphology of the CO+ and dust coma. The distributions of dust and CO+ ions in the coma are not similar and vary depending on the level of comet activity. CO+ ions are more concentrated towards the nucleus than the dust continuum. The column density of the CO+ was derived and found to vary from 3.7 × 109 to 4.3 × 1010 ions cm–2. The production rate of CO+ was estimated to be from (7.01 ± 2.7) × 1024 to (1.15 ± 0.5) × 1026 ions s–1. Processing the solar wind parameters (calculations based on the NASA CCMC ENLIL solar wind model) provided a close to linear dependence of the ionization rate on the solar wind ion flux, which suggests that impact ionization by solar wind particles is the main ionization mechanism at large heliocentric distances.

[1] Ivanova, O., Agapitov, O., Odstrcil, D., Korsun, P., Afanasiev, V., & Rosenbush, V. (2019). Dynamics of the CO+ coma of comet 29P/Schwasmann–Wachmann 1. *Monthly Notices of the Royal Astronomical Society*, *486*(4), 5614–5620. https://doi.org/10.1093/mnras/stz1200

Photometric studies of small bodies of the Solar System

S.A. Borysenko[1], O.R. Baransky[2], V.V. Kleshchonok[2]

[1]Main astronomical observatory, National Academy of Sciences of Ukraine, Kyiv, Ukraine
[2]Astronomical observatory of Taras Shevchenko National University, Kyiv, Ukraine

We present the results of the photometric studies of different groups of minor bodies (main belt active objects, quasi-Hilda comets, quasi-Trojan comets, trans-Jupiter comets) during of last years. A wide range of physical characteristics (absolute magnitudes, radii of comet nuclei, color indices, dust productivity parameters) for various cometary subgroups were obtained. A morphological analysis of images of comets with orbits at heliocentric distances of 2–6 a. u. was also carried out. A study of more than 25 comets from 2012 – 2021 demonstrates some differences in physical properties (dust production parameter, color indices) for different dynamical groups.

We also present MPC statistics of broadband (R-band) photometric monitoring for asteroids and comets at Kyiv comet station (MPC code – 585) for the last years, which include potentially dangerous asteroids approaching the Earth. Information about discovered and rediscovered objects is presented.

The long-lasting activity of asteroid (248370) 2005 QN173

O. Ivanova[1,2,3], I. Luk'yanyk[2], Marek Husárik[3]

[1]Main Astronomical Observatory of the National Academy of Sciences of Ukraine, Ukraine
[2]Astronomical observatory, Taras Shevchenko National University of Kyiv, Ukraine
[3]Astronomical Institute of the SAS, Slovak Republic

The results of imaging photometric, polarimetric, and long-slit spectroscopic observations of active asteroid (248370) 2005 QN173 are presented. The active asteroid showed long-lasting activity with a compact coma and long dust tail from July to December 2021. The dust production was estimated as Afρ near 20 cm in the r-sdss filter. Average values of the polarization respect to the typical value of polarization observed for C-type asteroids. No emission lines were detected. Using our observations of the asteroid, we will attempt to model the physical characteristics of the dust particles in the coma and tail.

Complex study of comet C/2013 X1 (PANSTARRS)

O. Shubina[1,2], O. Ivanova[1,3,2], I. Luk'yanyk[3]

[1]Main astronomical observatory of National academy of sciences of Ukraine, Kyiv, Ukraine
[2]Astronomical institute of Slovak academy of sciences, Tatranská Lomnica, Slovakia
[3]Astronomical observatory of Taras Shevchenko national university of Kyiv, Kyiv, Ukraine

We present the results of complex (photometric, spectral, and polarimetric) observations of hyperbolic comet C/2013 X1 (PANSTARRS). The observations were carried out on November 4, 2015, using the multi-mode focal reducer SCORPIO-2 attached at the primary focus of the SAO RAS 6-m telescope BTA. The comet demonstrated typical red V-R colour. We estimated dust productivity of about 1600 cm using Afρ proxy. Distribution maps of intensity and degree of linear polarization were

constructed and revealed a non-uniform structure of the dust coma. CN, C_2, C_3, and NH_2 molecule-emission features were detected in the cometary spectrum.

Transit photometry of planetary systems of WASP, TrES, Qatar and Kepler projects in Kyiv Comet Station (Lisnyky)

A. Nahurna[1], M. Solomakha[1], M. Lobodenko[1], O. Baransky[2]

[1]Taras Shevchenko National University of Kyiv, Ukraine
[2]Astronomical Observatory of Taras Shevchenko National University of Kyiv, Ukraine

We report the results of investigation of five planetary systems TrES-3b, Kepler-17b, WASP-3b, Qatar-1b, and Qatar-2b. Observations were carried out from 2 April 2021 to 14 February 2022 by using the 70-cm reflecting telescope AZT-8 of the Astronomical Observatory of Taras Shevchenko National University of Kyiv /Kyiv comet station. Photometric processing of the observation results was performed by using the Muniwin program. The obtained exoplanet transit brightness curves were published in Exoplanet Transit Database (ETD). The accuracy and quality of our observations on the ETD database scale ranged from 1 to 3.

For the exoplanets TrES-3b, Kepler-17b, WASP-3b, and Qatar-1b the obtained results of the center-transit time, depth and length of transit agree with the ephemeris data of ETD, while for observations of the Qatar-2 system for the planet Qatar-2b there is a clear decreasing trend of the value of the O-C parameter.

Additionally, applying the method of time transit variation (TTV) to our and Exoplanet Transit Database (ETD) data, we found a possible gravitational effect on the orbit of the exoplanet Qatar-2b of another massive body. This suggests that the assumption of the existence of the planet Qatar-2c conjectured in Bryan et al. (2011) is true.

Observations of comet 67P/Churyumov-Gerasimenko in 2021-2022 at Kyiv Comet Station (MPC 585)

O. Pyshna[1], A. Baransky[1], S. Borysenko[2]

[1]Astronomical Observatory Taras Shevchenko National University of Kyiv, Ukraine
[2]Main Astronomical Observatory NAS of Ukraine, Ukraine

In this work, we are presenting the results of astrometric, photometric, and dust productivity analysis of comet 67P/Churyumov-Gerasimenko. The results are based on 14 nights of observations at the Kyiv Comet Station (MPC Code 585) during the near-perihelion and Earth approach periods of 2021-2022. We also analyzed the photometric and astrometric data of 67P comet appearance in the 1969-2022 period of observations published in Minor Planet Center and Comet Observation databases (COBS).

For observations, we used the 0.7 m (f/4) reflector AZT-8 with the FLI PL4710 CCD camera. Astrometrica and FindOrb software was used for astrometric analysis and orbital elements calculations, and Comet for Windows and FoCAs 3.70 software was used for photometric and dust productivity analysis. On the basis of our images, we have measured precise astrometrical positions, magnitudes of 67P in different apertures for all the period of our observations, and values of Afρ parameter for most of our observations.

Based on observations published in the MPC database, we calculated orbital elements of 67P during 11 epochs. Also, on the basis of the COBS database, we calculated photometrical parameters for comet appearances in 1982-2022 and analyzed the dynamics of their change. We checked the accuracy of our astrometric results by comparing them with MPC data from the last 6 months in FindOrb software. We sent the results of 7 nights of observations to the MPC database with O-C residuals less than 1″.4. Overall, 157 results of observations were published in MPC database, and the observations with the highest precision were published in Minor Planet Circulars. The RA (O-C) residuals of published results of observations vary from 0.02+ to 1.4- arcseconds and Declination (O-C) residuals vary from 0.01+ to 1.4+ arcseconds. The mean residuals of elements of 67P orbit, calculated considering gravitational and non-gravitational effects of A1 and A2 comet model, vary from 0″.87 to 0″.34. As a result of our photometric research, we measured that the photometric parameters of 67P for 2021-

2022 appearance are H0 = 9.59m and K = 5.65, and the values of the Afρ dust productivity parameter were changing from 102 cm (1 month before the perihelion) to 317 cm (2 months 2 weeks after the perihelion) without phase correction. As a result of our photometrical analysis, we report asymmetry between the maximum of apparent magnitude and the moment of perihelion.

ФІЗИКА СОНЦЯ ТА СОНЯЧНА АКТИВНІСТЬ

SOLAR PHYSICS AND SOLAR ACTIVITY

Flare activity and magnetic complexity of active regions during solar cycles 23–24

O.A. Baran[1], A.I. Prysiazhnyi[1]

[1]Astronomical Observatory of Ivan Franko National University of Lviv

We performed a statistical analysis of selected active regions (ARs) parameters during the solar cycles 23–24 in order to investigate their flare activity. We used data on active regions, including their magnetic complexity, and flares in them from the SolarMonitor database. We supplemented this dataset with information about solar flares obtained with the XRS instrument of the GOES satellite.

It is found that the solar flare occurrence rate depends on the area of AR and its class of magnetic complexity: the larger the area and the more complex the configuration of the magnetic field, the greater is the integral flux of soft X-ray radiation from flares in this region.

It is shown that the flare activity of ARs (flares of classes C, M, X) increases around the maximum phase of the solar cycle and significantly decreases during the solar activity minimum. Class B flares show a different type of cyclicity: the largest number of them was detected during the ascending and descending phases of solar cycle. On average, during the solar activity cycle, the following tendency is observed: the stronger the flares, the smaller percentage of them occur in ARs of the simple group, and the higher percentage – in ARs of the complex group.

In the solar activity maximum, at least for classes B and C, the relative number of flares that occur in ARs with a complex magnetic configuration increases. During this period, the relative number of X-class flares significantly prevails in the regions of the $\beta\gamma\delta$ magnetic complexity class.

Forecast of the maximum 25th cycle of solar activity based on data on the rate of increase in the number of sunspots

V.M. Efimenko[1], V.G. Lozitsky[1]

[1]Astronomical Observatory of the Taras Shevchenko National University of Kyiv, Ukraine

Solar activity is a rather complex phenomenon in the Sun's atmosphere, which has a magnetic nature and cyclical changes over time. Another, 25th cycle of solar activity is expected in 2024-2026. At present, reliable methods of forecasting solar activity have not yet been created, although there are quite a lot of scientific works on this topic. A comparison of the latest forecasts of solar activity in the new 25th cycle, which began in December 2019, shows that the state-of-the-art forecasting methods produce significantly different results. The current 25th cycle also draws attention to the fact that it is from it that one can conclude that the long-awaited minimum of the age cycle of solar activity is approaching, which falls around the middle of the 21st century.

The purpose of this work is to obtain a predictive estimate of the amplitude of the 25th cycle, based on the rate of increase in the number of sunspots during the growth phase of this cycle.

Based on data on 24 previous solar cycles, the statistical relationship between the rate of increase in the number of sunspots in the phase of the growth curve and the amplitude of the cycle was considered. It turned out that the result of forecasting the cycle amplitude depends on which part of the growth curve is taken as the basis for forecasting, as well as whether all 24 cycles are taken into account, or only the odd ones. The prediction result is also affected by the initial assumption about monotonicity or non-monotonicity of the growth phase. It was concluded that, most likely, the maximum smoothed number of sunspots in the 25th cycle should be equal to 185 ± 18 units in the new system, which corresponds to the average power of the solar cycle, with the implementation of the Gnievyshev-Ohl rule. With such parameters of this cycle, there are no signs of approaching the deep minimum of the age cycle in the middle of the 21st century.

Magnetic fields in a limb solar flare at a height of 40 Mm according to spectral-polarization observations in the Hα line

M.A. Gromov[1], I.I. Yakovkin[2] ,V.G. Lozitsky[2]

[1] Physical Faculty of the Taras Shevchenko National University of Kyiv, Ukraine
[2]Astronomical Observatory of the Taras Shevchenko National University of Kyiv, Ukraine

We present the results of measurements of the magnetic field in the solar flare of July 19, 2012 of M7.7 score based on the data of spectral-polarization observations made on the Echelle spectrograph of the horizontal solar telescope of the Astronomical Observatory of Taras Shevchenko Kyiv National University. The material of the observations was a Zeeman spectrogram from 6:45:50 UT, which was scanned using the Epson Perfection V 550 scanner. The blackening was converted into intensity taking into account the characteristic curve of the photomaterial of the spectrogram and the nonlinearity of the scanner itself. To measure the Zeeman splittings, the I+V and I-V spectra were "tied" by wavelengths using telluric lines. It was established that the averaged (effective) magnetic field B_eff in this flare reached 600-700 G, but local magnetic fields could be much stronger. The inhomogeneity of the magnetic field is evidenced by the following effects: (a) the splitting of the bisectors of the I+V and I-V profiles is unequal at different distances from the center of the emission profile of the H-alpha line - in general, this splitting increases from the wings of the emission profile of the H-alpha line to its core, (b) at distances from the center of 350-450 mA, a local maximum of bisector splitting is observed. Effect (b) is possible with extremely strong magnetic fields at the level of 10^4 G, but this result needs careful verification.

Probing the upper solar corona using spectral imaging observation with LOFAR

Mykola Gordovskyy[1]

[1]University of Hertfordshire, UK

The upper solar corona is difficult to probe: its density is too low to produce detectable bremsstrahlung X-ray emission, while the magnetic field is usually too weak to yield observable gyro-synchrotron microwave emission. This makes low-frequency plasma emission induced by propagating energetic electrons an essential diagnostic tool for the physical conditions in the upper atmosphere of the Sun. The Low-frequency Radio Array (LOFAR) offers an opportunity to observe spatially resolved radio-emission of the Sun with high frequency resolution. The tied beam-array mode also makes it possible to observe the Sun with high temporal cadence (with the resolution of less than 100ms), which is essential for capturing fast variations of the radio-emission in the solar radio bursts. I will discuss recent progress in understanding low-frequency radio-emission of the Sun made using LOFAR data. In particular, I will focus on the spatial characteristics of emission sources in solar radio bursts (locations, sizes and shapes, apparent motions) and how these characteristics are used to probe the density structure, plasma turbulence and magnetic field topology in the upper corona [1,2].

References:

[1] D.L. Clarkson et al. 2021 ApJ Lett., 917, 32.
[2] M. Gordovskyy et al. 2022, ApJ

Unusual solar active region

N.M. Kondrashova[1], V.N. Krivodubskij[2]

[1] Main Astronomical Observatory, National Academy of Sciences of Ukraine, Kyiv, Ukraine
[2]Astronomical Observatory of Taras Shevchenko National University of Kyiv, Kyiv, Ukraine

Unusual active region NOAA 13088 was observed in the solar disk on August 2022. This active region violates Hale's law. Its magnetic field poles are rotated 90 degrees compared to other active regions.We have analyzed the evolution of this active region, using data from space observatories. The full-disk magnetograms, continuum images and EUV-images were provided by the Solar Dynamics Observatory (SDO) the Helioseismic and Magnetic Imager (HMI) and the Atmospheric Imaging Assembly (AIA). The X-ray data were obtained at Geostationary Operational Environmental Satellite (GOES).

The active region NOAA 13088 appeared in the southern hemisphere of the solar disk on 24 August 2022 and was observed in the solar disk from 24th to 30th of August 2022.The structure of the region was changing. The number and area of spots increased.The complexity of the magnetic field was increasing rapidly. The active region studied produced many events, including flares, jets, CMEs.On 27th of August SDO recorded the shock wave through the solar atmosphere from an M4- class flare. SOHO coronagraphs have detected a CME from the flare site.The flare M6.7-class on 28th August caused a CME and a shortwave radio blackout over the Americas. STEREO recorded power CME from the site of the region studied on the farside of the Sun on 5th September.

The active region 13088 has returned on 13th September and has been renumbered as NOAA 13102. The magnetic field configuration simplified. The sunspot number and the area of the active region increased again on 17th September. The flare activity of the region increased. The region went beyond the limb on 25th September.

A possible mechanism contributing to the appearance of the NOAA 13088 anti-Hale active region is discussed.The essence of solving the problem is as follows.In work [1], based on the processing of observational data for 1920-2004 from the Mount Wilson Catalog, it was found that in the "royal zone" a small number of bipolar groups of sunspots, which had the

"wrong magnetic polarity", were always observed.The authors of the study [1] called them "violators of Hale's law." They believe that the appearance of anti-Hale bipolar groups is related to changes in the mode of operation of the turbulent dynamo in the solar convective zone (SCZ). The large-scale (regular) magnetic field in the dynamo is inevitably accompanied by fluctuating magnetic fields excited by the small-scale dynamo in the depths of the SCZ. Therefore, during observations on the solar surface, a superposition of regular and fluctuating toroidal fields is usually recorded. At certain periods of time, the fluctuating magnetic component, which is oriented antiparallel to the regular component, may accidentally be so strong that it will exceed the magnitude of the magnetic induction of the regular component. As a result, the total magnetic field will violate Hale's law of polarity. We assume that the emergenceof the NOAA 13088 anti-Hale active regionwas associated with the mentioned accidental changes in the turbulent dynamo regime in the SCZ.

1.Sokoloff D., Khlystova A., Abramenko V. Solar small-scale dynamo and polarity of sunspot groups// MNRAS. – 2015. –V.451. – P. 1522–1527.

Observations of wave motions in the solar facula

R. Kostyk[1], N. Shchukina[1]

[1]Main Astronomical Observatory, National Academy of Sciences of Ukraine, Kyiv

The results of spectropolarimetric and filter observations of the facular region in the lines Fe I 1564.3, Fe I 1565.8 nm, Ba II 455.4 nm, and Ca II H 396.8 nm obtained near the solar disk center at the German Vacuum Tower Telescope (Tenerife, Spain) are discussed. It is shown that the facular contrast measured at the Ca II H line center first grows more and more slowly with magnetic field strength, and then, with its further increase goes down. The reason for this is the nonlinear height dependence of the line source function caused by a deviation from local thermodynamic equilibrium. It was found that waves propagating both upward and downward can be observed in any area of the facula, regardless of its brightness. Moreover, in bright areas with the strong magnetic field, upward waves dominate, while in less bright areas with the weaker field, downward waves are more often observed. The facular contrast measured at the center

of the Ca II H line is shown to correlate with the power of the wave velocity oscillations. In bright areas, it grows with the power, it does not matter in which direction the waves are propagating. In the areas with low brightness, the opposite dependence is observed for both types of waves. The power of the wave velocity oscillations, in turn, is sensitive to the magnetic field strength. In the facular bright magnetic elements the stronger the field, the higher the power of oscillations for both upward and downward waves. In the case of reduced brightness, the inverse relationship is observed. We conclude that the increase in contrast with the wave velocity power which is observed in the bright facular regions can be considered as evidence that these areas look bright not only because of the Wilson depression, but also owing to heating of the solar plasma by waves.

Long-term variations of solar magnetic activity

V. N. Krivodubskij

Astronomical Observatory of Taras Shevchenko National University of Kyiv

The main law of the evolution of the Earth's climate is the cyclical nature of global changes in the latter. One of the possible explanations for the cyclical nature of global climate changes is provided by the astrophysical model of fluctuations in the insolation of the Earth's surface by solar radiation. Modern climate change is mainly associated with variations in the magnetic activity of the Sun, one of the main proxies of which are sunspots. The decrease in the number of sunspots coincides with the epochs of cooling on the Earth, while during the maximum number of sunspots warming is observed. The paper reviews cosmogenic reconstructions of long-term variations in the Sun's magnetic activity (large minima and large maxima) during the Holocene (last 12,000 years). The accidental appearance of large minima and maxima can to some extent be reproduced by modern models of a turbulent dynamo with a stochastic drive.

An important key to studying the impact of solar activity variations on the Earth's climate is the Maunder minimum (late 17th century), during which extremely little sunspots were observed. Applying the method of analysis of rare events to these observations led researchers to conclude that the appearance of sunspots at the Maunder minimum was characterized by a

weak amplitude of 22 years. The concept of continuity of magnetic cycles at this time is also confirmed by measurements of cosmogenic radionuclides in natural terrestrial archives. Therefore, today it is believed that during the Maunder minimum, the cyclic magnetic activity of the Sun did not stop, although the amplitude of the cycles was quite low. In the αΩ-dynamo model, this may be due to the fact that the magnitude of the magnetic induction of the toroidal field excited by radial differential rotation in the SCZ at this time did not reach the threshold value required for lifting magnetic power tubes on the solar surface (nonlinear dynamo mode). Possible physical mechanisms describing the suppression of the dynamo process at intervals when no sunspots were observed are analysed.

A scenario for explaining the north-south asymmetry of magnetic activity during the Maunder minimum is proposed. A key role in the proposed scenario is played by the special nature of the internal rotation of the Sun, revealed as a result of helioseismological experiments.

The modern grand maximum of solar activity, which began in the 1940s, has ceased after solar cycle 23, and activity of the Sun seems to be returning to its normal moderate level.

Kinematic dynamo model of solar magnetic cycle

A.A. Loginov[1], O.K. Cheremnykh[1], V.N. Krivodubskij[2], Y.O. Selivanov[1]

[1]Space Research Institute, National Academy of Science of Ukraine
[2]Astronomical Observatory of Taras Shevchenko National University of Kyiv

The report deals with the problem of explaining the origin and nature of the space-time variations in the magnetic activity of the Sun. The paper presents new hydrodynamic model of the solar magnetic cycle, which uses helioseismological data on the differential rotation of the solar convective zone. The model is based on the hypothesis of the emergence of global flows as a result of the loss of stability of a differentially rotating plasma layer in the convective zone. First, the hydrodynamic global plasma flows are calculated without taking into account the effect of a magnetic field on them. Under this condition, it is shown that the solutions found describe all global flows observed on the surface of the Sun: permanent meridional circulation from the equator to the poles, torsional oscillations and space-

time variations of the meridional flow. The report concludes that the last two flows are azimuthal and meridional components of a single three-dimensional global hydrodynamic flow. Second, to simulate the dynamics of the magnetic field, the found velocities of global migrating flows and the spatial profile of the angular velocity of the internal differential rotation of the solar convective zone obtained from helioseismic measurements were used. Good coincidences have been obtained between the characteristics of the calculated dynamics of global migrating flows and the variable global magnetic fields generated by them with the observed values on the solar surface. An explanation is given for some phenomena on the surface of the Sun, which could not be explained within the framework of the existing models.

Relationship between major geomagnetic storms and changes in the Mean magnetic field of the Sun

N.I. Lozitska[1]

[1]Taras Shevchenko National University of Kyiv, Ukraine

A study of Solar Mean magnetic field changes before major geomagnetic storms was carried out. To fill in the observational gaps, the relationship of the Stanford SMMF data with the Mean total magnetic flux observed by the SOLIS VSM was investigated. The analysis of the obtained continuous series of data was carried out. A significant decrease in the **Solar Mean magnetic field** was detected 3-10 days before the start of a geomagnetic storm. The magnitude of this decrease correlates with the planetary geomagnetic storm indices.

Search for superstrong magnetic fields in sunspots using spectral lines with various Lande factors

V.G. Lozitsky [1], S.M. Osipov [2], M.I. Stodilka [3]

[1] Astronomical Observatory of the Taras Shevchenko National University of Kyiv, Ukraine
[2] Main Astronomical Observatory of National Academy of Science, Kyiv, Ukraine
[3] Astronomical Observatory of Ivan Franko National University of L'viv, L'viv, Ukraine

The spectra of two sunspots of July 8, 2015 and September 5, 2021 were analyzed using observations with the ATsU-5 solar telescope of the Main Astronomical Observatory of the National Academy of Sciences of Ukraine. The main goal of the study was to search for signs of superstrong magnetic fields in sunspots (> 10^3 G), taking into account the fact that such magnetic fields can have mixed magnetic polarity. An SBIG ST-8300 CCD camera was used to record a spectral interval of about 8 Å near the Fe I 5434.5 Å line, where six metal lines with effective Lande factors g_{eff} from –0.014 to 2.14 are located. Also, FeI 5397.1 line with $g_{\text{eff}} = 1.426$ was studied too for second sunspot. In the first spot, we found a splitting of the $I \pm V$ profiles in the FeI 5434.5 line, corresponding to a magnetic field with a strength of ≈ 25 kG, which has the opposite magnetic polarity with respect to the "kilogaussian" magnetic field (≈ 2 kG) determined from lines with large Lande factors. A detailed comparison of the spectral widths in the Stokes *I* profiles of two lines of the 15th iron multiplet, FeI 5434.5 and 5397.1 Å, showed that their additional widening (local peaks of splitting) sometimes occur at different places on the Sun. Considering that these lines have almost the same temperature sensitivity and formation height in the atmosphere, it is unlikely that this is a non-magnetic effect due to variations in thermodynamic conditions and velocity field. Regarding the possible influence of spectral blends, the paradox is that it is the more "clean" line Fe I 5434.5 that demonstrates the most incomprehensible splitting peaks. This strengthens the assumption that the observed splitting peaks are of a magnetic nature. But then, if we assume that the additional widening of the 5434.5 line is due to the magnetic field, then its value should be ~ 10^5 G. The semi-empirical model for the first sunspot was build using so-called Tikhonov stabilizers, which modify the objective function, to ensure the

smoothness and stability of the solutions of the inverse problem. This model has an anomalous feature, namely, the maximum of micro-turbulent velocities in the region of the temperature minimum, i.e. where the minimum of these velocities presents in the model of a quiet photosphere. Perhaps this feature indicates very strong magnetic fields in this sunspot. On the whole, we cannot draw a final conclusion about the existence of the named superstrong magnetic fields in sunspots, but we draw attention to interesting and mysterious effects in the line profiles, which require additional studies.

The modulus of the Mean magnetic field of the Sun as an index of space weather

O.V. Muryniuk[1], N.I. Lozitska[1]

[1]Taras Shevchenko National University of Kyiv, Ukraine

Variations of the average annual components of the interplanetary magnetic field in cycles of solar activity were studied. A close relationship between the average annual values of the interplanetary magnetic field on the Earth's orbit and the module of the Solar Mean magnetic field has been revealed. It is shown that the correlation coefficient between the interplanetary magnetic field and the sunspot index is significantly smaller than with the module of the Solar Mean magnetic field. This difference is due to the delay of maximum and the descending branch of the magnetic fields of the Sun and interplanetary space relative to the number of spots in the cycles of solar activity. The modulus of the Solar Mean magnetic field can be used as an index of long-term changes in solar activity.

The dynamical features of a solar surges in an emerging flux region

M.N. Pasechnik

Main Astronomical Observatory, NAS of Ukraine, Kyiv, Ukraine

We present the results of studying the features of Hα-ejections (surges) formation and development arose on a site of the NOAA 11024 active region. The work was performed on the basis of spectral data with high spatial (below 1 arcsec) and temporal resolution were obtained with the THEMIS French–Italian 90-cm vacuum telescope (Tenerife, Spain) on July 4, 2009. The observation time was 20 minutes ($9^h52^m35^s$ to $10^h11^m26^s$), 400 Hα spectra with a time interval of ~ 3 seconds were obtained. From them, we used 36 spectra of the best quality. Stokes I profiles were obtained, with an interval corresponding to 160 km on the surface of the Sun.

The area under study (its length was 10 Mm) was in the region of emerging a new magnetic flux in the form of a serpentine magnetic field. As a result its interaction with the surrounding already existing magnetic field, a pore was formed, an Ellerman bomb developed at a distance of about 7.2 Mm from it, and Hα-ejections occurred. In all spectra, surges were visible in the absorption. At the beginning of the observations for 13 minutes, surges were visible only in the short-wavelength wings of the Hα line. Depending on whether the ascending or descending motion of the chromospheric matter was observed in the serge, the serge profile component was projected onto the blue or red wing of the Hα line. Doppler shifts of these components were used to calculate the line-of-sight velocities (Vlos) of chromospheric matter in surges. The intensity of this component sometimes exceeded that of the main component. Sometimes two components with two distinct minima were clearly identified in the Hα profiles. In these cases, the position of both minima has been measured. The dynamics of surges during their evolution were studied: the temporal changes in the line-of-sight velocities of plasma and the direction of its movement. Changes in the velocity of of the chromospheric matter movement along the cross section at the site of the maximum intensity of the ejection were also determined. The size of the cross section of the ejection also changed, with time it increased.

It was found that in most cases the surges occurred at a high velocity - plasma Vlos up reached -95 km/s, and down - 80 km/s. Over time, the Vlos decreased, but the plasma moved along the magnetic loop unevenly -

sometimes slowing down, then speeding up. The velocity distribution in the surges indicates their multi-flow structure - they consisted of several chromospheric matter jets that arose during reconnection. The jets velocity was different and probably depended on the structure of the magnetic field in the surge and the surrounding environment. One of the surges, which formed near the Ellerman bomb, showed signs of plasma vortex motions, as evidenced by the inclined dark streaks in the spectra. Their incline has decreased over time. At some moments, on a small area of about 160 - 250 km (1 - 1.5 pixels in the spectrum), there was a sharp change in the velocity and direction of movement of the chromospheric matter - two oppositely directed flows could exist side by side. On the spectra obtained at the end of the observations, the central part of the Hα line was completely covered by dark details. This means that the plasma movement occurred in the upper parts of the magnetic loops. The Vlos at this time changed from -20 km/s to 15 km/s.

The spectra can very well trace the surges evolution features of from their appearance to their disappearance, if the limited time of observation allowed it. A dark detail appeared in the short-wavelength wing of the Hα line, which over time gradually moved to the core of the line, superimposed on it, and began to move to the long-wavelength wing. Indicating that the surge, moving up the magnetic loop, has reached a certain height, or the upper part of the loop, and under the influence of gravity has begun to descend along a path close to that by which it ascended, or along the other side of the loop.

The obtained results can be used in the verification of existing and creation of new theoretical models of Hα-surges.

Features of the manifestation of space weather in the area of the location of the radio telescope "URAN-4" RI NASU and the Odessa magnetic anomaly

M. Ryabov[1], M. Orlyuk[2], A. Sukharev[2], A. Romenets[1], L. Sobitniak, V. Komendant[1], V. Galanin[1], V. Derevyagin[1]

[1] Odessa observatory « Uran-4» Institute of Radio Astronomy of the NAS of Ukraine, Ukraine
[2] Institute of Geophysics of the NAS of Ukraine, Ukraine

Space weather in the growth phase of the 25 solar cycle is realized in the form of various "scenarios" determined by the manifestations of solar activity. Among them are the presence of solar flares and coronal mass ejections, particle flows from solar coronal holes. There are periods when these events follow one after the other or occur simultaneously. Radio telescope "URAN-4" of the Odessa Observatory of the Radio Astronomy Institute of the NASU is located near the Odessa Magnetic Anomaly (OMA). Odessa Regional Magnetic Anomaly is the largest in Ukraine. It has a number of interesting properties that determine its reaction to the manifestations of solar and geomagnetic activity. OMA extends to altitudes of about 90-100 km, which can affect the dynamics of processes in the ionosphere during periods of magnetic storms. To clarify the dependence of the results of radio astronomical observations on the time of appearance of magnetic storms according to the data of the magnetic observatory "Odessa" of the Institute of Geophysics of the NASU (IG NASU) in the village of Stepanovka, a catalog of magnetic storms was compiled for the period of operation of the radio telescope in 1987 - 2009. The results of the catalogue studies showed a longer duration of magnetic storms in the OMA zone compared to the higher-latitude magnetic observatory IZMIRAN. From 2017 to 2022, magnetometric observations were carried out at the OMA center in Shevchenko Park on the territory of the astronomical observatory of ONU named after I.I. Mechnikov. The data of these measurements were compared with the results of observations at the magnetic observatory "Odessa" located in the south-eastern part of the anomaly. They showed a number of differences in the manifestation of short-term variations in magnetic storms in the center and at the edge of the OMA. Since July 2022, the magnetometer has been installed in the immediate vicinity of the Uran-4 radio telescope in the village of Mayaki, Odessa region, to conduct joint

radio astronomical and magnetometric studies. Examples of the development of various periods of solar activity in 2022 are presented.

The results of the features of the manifestation of short-period variations of the XYZ component of the geomagnetic field, which occurred during various phenomena of solar activity and magnetic storms, are given. The presence of previously little-known stable geomagnetic variations with a basic period of about 2 minutes and two harmonics of the main period (1 minute and 30 seconds) was revealed. In addition, the change in the amplitude and periods of diurnal harmonics (6, 4, 2 hours) during magnetic storms was investigated. The presence of previously little-known stable geomagnetic variations with a basic period of about 2 minutes and two harmonics of the main period (1 minute and 30 seconds) was revealed. In addition, the change in the amplitude and periods of diurnal harmonics (6, 4, 2 hours) during magnetic storms was investigated.

Signatures of possible superstrong magnetic fields in a limb solar flare and an active prominence from polarization study of Ha and He I D3 spectral line profiles

I.I. Yakovkin[1], V.G. Lozitsky[1]

[1]Astronomical Observatory of the Taras Shevchenko National University of Kyiv, Kyiv, Ukraine

We report the signatures of possible 10^5 Gauss magnetic fields in the 14 July 2005 limb solar flare. During the post-peak phase of the flare, such strong fields are observed at altitudes between 10 and 20 Mm, manifesting as strongly split peaks (up to 4 Å apart in wavelength) in the far wings of the Ha emission. The analysis of the Stokes V profiles reveals the presence of a large antisymmetric circular polarization relative to the center of the broad emission. The shape of the Stokes V profiles differs significantly from the dI/dl intensity gradient profiles, indicating the presence of a strong magnetic field. In the He I D3 line, similar spectral features were also seen for a prominence on 12 July 2004 at heights up to 25 Mm. If these spectral features are viewed as indications of the Zeeman effect, the corresponding magnetic fields can be as strong as 130 kG. Notably, such spectral features are extremely rare and are absent from the spectra of the vast majority of flares and prominences, as we demonstrate by analyzing the spectrum of an active prominence on July 24, 1999.

To explore the possibility of interpreting such highly split spectral features as manifestations of extremely powerful magnetic fields, we conducted a theoretical analysis of the dependence of line profiles on magnetic fields of different strengths. The calculations show that at such extremely high magnetic fields, the fine structure of the spectral lines leads to profile shapes that are similar to those seen. This suggests that the patterns seen in the Stokes V profiles can indeed be a sign of extremely strong magnetic fields.

Comparison of solar activity proxies: eigen vectors versus averaged sunspot numbers

V.V. Zharkova[1,2⋆], I. Vasilieva [2,3], S.J. Shepherd[4] and E. Popova[5]

[1]Department of MPEE, University of Northumbria, Newcastle upon Tyne, UK
[2]ZVS Research Enterprise Ltd., London, UK
[3]Department of Solar Physics, Main Astronomical Observatory, Kyiv, Ukraine
[4]PRIMAL Research Group, Sorbonne Universite, Paris, France
[5]Centro de Investigacio´n en Astronom´ıa, Universidad Bernardo O'Higgins, Santiago, Chile

We attempt to establish links between a summary curve, or modulus summary curve, MSC, of the solar background magnetic field (SBMF) derived from Principal Component Analysis, with the averaged sunspot numbers (SSN). The comparison of MSC with the whole set of SSN reveals rather close correspondence of cycle timings, duration and maxima times for the cycles 12- 24, 6,7 and -4,-3. Although, in 1720-1760 and 1830-1860 there are discrepancies in maximum amplitudes of the cycles, durations and shifts of the maximum times between MSC and SSN curves. The MSC curve reveals pretty regular cycles with double maxima (cycles 1-4), triple maximum amplitude distributions for cycles 0 and 1 and for cycles -1 and -2 just before Maunder minimum. The MSC cycles in 1700-1750 reveal smaller maximal magnitudes in cycles -3 to 0 and in cycle 1-4 than the amplitudes of SSN, while cycles -2 to 0 have reversed maxima with minima with SSN. Close fitting of MSC or Bayesian models to the sunspot curve distorts the occurrences of either Maunder Minimum or/and modern grand solar minimum (2020-2053). These discrepancies can be caused by poor

observations and by difference in solar magnetic fields responsible for these proxies. The dynamo simulations of toroidal and poloidal magnetic field in the grand solar cycle (GSC) from 1650 until 2050 demonstrate the clear differences between their amplitude variations during the GSC. The use of eigen vectors of SBMF can provide additional information to that derived from SSN that can be useful for understanding solar activity.

ДОСЛІДЖЕННЯ АТМОСФЕРИ ТА ІОНОСФЕРИ

ATMOSPHERE AND IONOSPHERE RESEARCH

Ionospheric Effects of Powerful Typhoons Over the PRC: Results of Oblique Sounding

L.F. Chernogor[1,2,3], K.P. Garmash[1], Q. Guo[2], V.T. Rozumenko[1], Y. Zheng[3]

[1]V. N. Karazin Kharkiv National University, Kharkiv, Ukraine
[2]Harbin Engineering University, 145 Nantong Street, Nangang District, Harbin, 150001 China
[3]Qingdao University, 308 Ningxia Road, Qingdao, 266071 China
vtrozumenko45@gmail.com

The scientific objectives of this study is to experimentally and theoretically study the ionospheric response to powerful tropospheric phenomena (typhoons) occurring in the north-western Pacific.

Instrumentation. The HF radio system has been created in collaboration between the Chinese and Ukrainian researchers utilizing software-defined radio technology permitting high-quality scientific measurements. The receiver system is located at the Harbin Engineering University campus (43.78˚N, 126.68˚E), and the transmitters of 14 broadcasting radio stations are found in the range of 910–1,875 km from Harbin in Japan, Mongolia, the Russian Federation, the Republic of Korea, and the PRC.

Basic information on the typhoons under study. We have chosen three typhoon events viz Lingling, Faxai (September 1–10, 2019), and Hagibis (October 6–13, 2019) to study disturbances in the electron density and the basic features of the variations in radio wave characteristics. The maximum pressure deficit in Typhoon Lingling was ~65 hPa, the largest radius of the storm and gale wind wasre 170 km and 560 km, respectively, along the typhoon path of 3,750 km. The typhoon kinetic energy and power are estimated to be 5.5×10^{17} J and 5.5×10^{12} W. The maximum pressure deficit in Typhoon Faxai was ~52 hPa, while its energy and power were estimated to be 1.8×10^{17} J and 1.3×10^{12} W. The Typhoon Hagibis has been the strongest typhoon for over 60 years. Its pressure deficit attained 95 hPa and energy and maximum power were estimated to be 5.5×10^{18} J and 1.1×10^{14} W.

Wave effects in the ionosphere. Part of the tremendous typhoon mechanical energy and power, via quite a long and complicated chain of transformations, eventually launches atmospheric gravity waves and infrasound in the neutral atmosphere, which modulate the electron density.

Consequently, the Doppler spectra and the Doppler shifts are observed to exhibit regular (quasi-sinusoidal) and chaotic variations. The action of the Typhoon Lingling on the 6/7 September 2019 night was accompanied by a 23% reduction in the *F*-region electron density. The action of the Typhoon Faxai during the 9/10 and 10/11 September 2019 nights was accompanied by a 27% decrease in the ionospheric *E*- and *F*-region electron densities. The ionospheric *F*-region electron density was enhanced by 56% on the 8/9 September 2019 night when the Typhoon Faxai came closest to the ionosonde and had the highest energy. The amplitude of the quasi-sinusoidal variations in the ionospheric *F*-region electron density under the action of the Typoon Hagibis was estimated to be 10–12% for periods of ~20 min, and 30–60% for periods of ~60–120 min, while the amplitude of the quasi-sinusoidal variations in the electron density varied in the 0.2–0.4% range in the infrasonic period range. On 9 October 2019, the height of the reflection level was observed to oscillate within the 30–50 km to 60– 90 km limits.

Perturbations in Doppler shift and spectra. On 6 September 2019, the Typhoon Lingling action caused chaotic and quasi-sinusoidal variations in the Doppler shift, and a substantial, from −1 to 1 Hz and greater, broadening in the Doppler spectra. Synchronous quasi-sinusoidal variations in the signal amplitude have been detected with a peak-to-peak amplitude of 10 dBV and a period of 7 min; these variations arise from radio ray focusing/defocusing caused by the quasi-sinusoidal electron density variations produced by the action of infrasonic waves launched by the Typhoon Hagibis.

Conclusion. Powerful typhoons act to enhance wave activity in the neutral atmosphere and plasma, to shift the heights of reflection levels by up to tens of kilometers, to cause significant (±1.5 Hz) Doppler spectrum broadening, and to cause multi-hop and multi-ray propagation of radio waves.

Temporal and spatial variations of the vertical distribution of ozone in mid-latitude satellite and Umkehr measurements

Yu. Andrienko[1], G. Milinevsky[1,2], Yu. Pryadko[1], M. Reshetnyk[1]

[1]Physics Faculty, Taras Shevchenko National University of Kyiv
[2]College of Physics, International Center of Future Science, Jilin University, Changchun, China
andrienko.j@gmail.com

In our work, we investigated temporal and spatial variations of the vertical ozone distribution for the period 2021-2022 at the middle latitudes of the Northern Hemisphere. The selected zone is within the range 48°-52°N and 0°-40°E. The work uses the data of measurements of the vertical distribution of ozone by the Aura MLS satellite instrument and own measurements of the vertical distribution of ozone obtained by the Umkehr method at the Kyiv Goloseyev Dobson station for comparison.

The analysis of satellite data confirmed the seasonal variations of ozone values in the maximum concentration, the increase of ozone values in the maximum for the winter and spring months. The range of ozone distribution values in the maximum concentration is 5-9.5·10^{-6}ppmv, which corresponds to a pressure of ~8 hPa. In winter, a significant spread in the values of ozone in the maximum concentration and quasi-wave fluctuations were found.

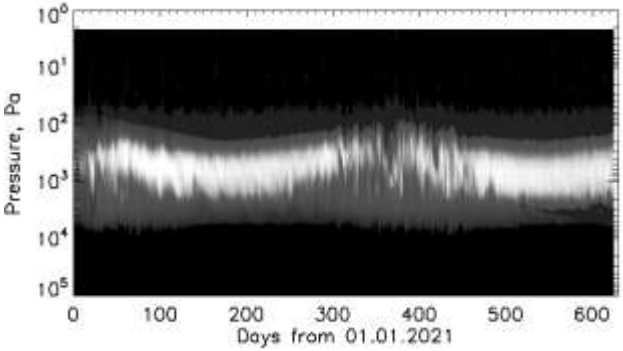

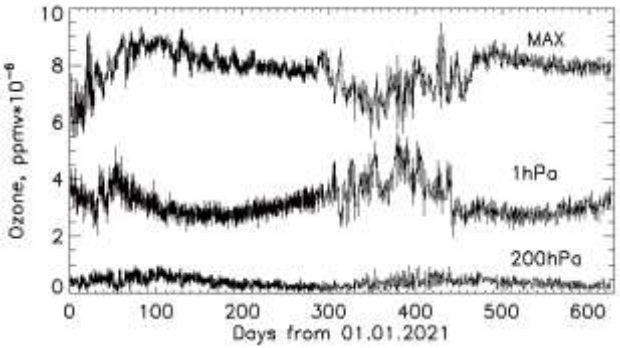

The analysis of spatial changes in the vertical distribution of ozone showed the presence of periodic maximum values of the amount of ozone in the maximum concentration in the winter period. The method of Phase dispersion minimization and Lomb Normalized Periodogram analysis was used to search for periodicity. The frequency of occurrence of maxima is about 2° in the range 0°-40°E.

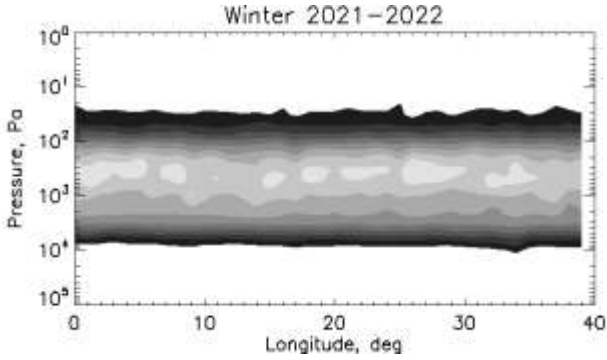

A comparison of the vertical profiles obtained by the MLS and the Umkehr method was also carried out.

This work was partly supported by the projects 20BF051-02 and BF/30-2021Taras Shevchenko National University of Kyiv. Part of this research was performed at the International Center of Future Science, Jilin University (JLU), under the contract with the JLU.

Fractal analysis in space physics

L.F. Chernogor[1], O.V. Lazorenko[1], A.A. Onishchenko[2]

[1]V. N. Karazin Kharkiv National University, Kharkiv, Ukraine
[2]Kharkiv National University of Radioelectronics, Kharkiv, Ukraine
oleg.v.lazorenko@karazin.ua

According to the non-linear and the system paradigms, many processes generated in open, non-linear, dynamical systems under influence of a powerful source of energy release are appeared to be short-time, ultra-wideband, non-linear and fractal. In applied physics, there are a lot of such processes and such systems. Therefore, to investigate the fractal properties of the signals and processes generated in the open, non-linear, dynamical systems, the set of corresponding methods are needed. Namely such modern and effective methods had been united in fractal analysis. Suddenly, but these methods are often appeared to be quite unknown for the most part of researchers, which work in space physics. No doubt, this state should be changed.

The purpose of this work is to draw attention of the researchers to the advantages of the fractal analysis methods, in particular, and to the fractal analysis application benefits, at all. To distinguish the purpose, the extended review of the existing fractal analysis methods applicable to investigations of the signal and processes of any origin is proposed. Please, note, this review deals with mono-fractal analysis only. Due to volume limitations of this paper, all existing multi-fractal analysis methods were appeared to be out of the scope of this work.

As a part of the fractal approach in nature created by the famous American researcher Benua Mandelbrot in 1970th, fractal analysis of the signals and processes unite a lot of methods based on calculation, first, of different fractal dimensions. Now there are over sixty methods, which are regularly applied in many branches of science and engineering, in particular, in the physics. As the theoretical bases of these fractal analysis methods, the concepts of one-parametric (the fractal Brownian motion and the fractional Gaussian noise) and multi-parametric (the generalized Cauchy process, the alpha-stable processes, including the Levi's flight, the generalized Ornstein-Uhlenbeck processes) mono-fractal signal models are used. All fractal dimensions calculated in the fractal analysis methods can be divided on two big groups. First of them is based on geometric properties of the signal

investigated. The second of them deals with statistical properties of the signal and their numerical characteristics (for example, with Hurst exponent). In the same time, all fractal analysis methods can be classified as simple (only one fractal dimension is used) and complex (the set of fractal dimensions is calculated) ones. First of them are appeared to be simpler to realize, second are appeared to carry more different and useful information. Let's take a quick look at the list of the most known simple fractal analysis methods. Today there are the Fourier dimension based method, the coarse graining spectral analysis method, the box-counting method, the real box-counting method, the differential box-counting method, the extended counting method, the multiresolution box-counting method, the Minkowski sausages method, the variation method, the Burlaga's and Klein's method, the Higuchi's method, the Katz method, the Petrosian's method, the Mandelbrot's method, the multiresolution length method, the Sevcik's method, the consecutive differences method, the normalized length density method, the critical exponent method, the average normalized autocorrelation method, the Maragos-Sun's method, the Renyi generalized dimensions method, the variational dimension method, the zero-crossing method, the Korcak's method, the Chens' method, the R/S-method, the Mandelbrot's and Wallis' method, the autocorrelation analysis method, the detrended fluctuation analysis, the detrended moving average method, the second moment method, the Peltier – Levi-Vehel's method, the variance plot method, the variogram method, the generalized variogram method, the aggregated dispersion method, the aggregated signal absolute values method, the periodogram method, the wavelet analysis based method, the empirical mode decomposition method, the dispersion analysis method, the signal summation conversion method, the regularization dimension method, the diffusion entropy analysis and other. As the complex fractal analysis methods, in particular, the generalized fractal analysis and the dynamical fractal analysis proposed by the authors of this paper can be considered. On our opinion, the correcting function method created this year by the same authors is appeared to be a useful addition to the all mono-fractal analysis methods. This method is an attempt to improve the accuracy of the fractal dimension estimations.

Work was supported by the National Research Foundation of Ukraine for financial support (project 2020.02/0015). Also this work was supported by Ukraine state research projects #0121U109881, 0121U109882, 0122U001476.

Electrical Effects of the Tonga Volcano Unique Explosion on January 15, 2022

L.F. Chernogor

V.N. Karazin Kharkiv National University, Kharkiv, Ukraine
leonid.f.chernogor@gmail.com

The purpose of this work is to describe the electrical effects in the troposphere and ionosphere caused by the explosion of the Tonga volcano on January 15, 2022. The mechanisms of electrical phenomena within the volcanic plume and at ionospheric heights are different. We will consider them separately.

Electrical effect in the troposphere. Under undisturbed conditions, the volume density of the electric charge is of order of 10^{-10} C/m^3. In the troposphere, the specific electrical conductivity is $2\cdot10^{-14}$ $\Omega^{-1}\cdot$m^{-1}. There is a vertical electric current, the density of which is $3\cdot10^{-12}$ A/m^2. The electric field strength is about 100 V/m. A volcanic eruption leads to an abrupt change in the electrical state of the atmosphere within the plume. Materials produced by volcanic eruptions significantly activate the processes of electrification and charge separation, generate an increase in the electric current, etc. Dust particles and aerosols play the main role. The mechanisms of particle electrification are primarily associated with the spraying of the substance injected into the atmosphere. The hot upward flow of the eruption materials, the speed of which gradually decreases from ~100 to ~10 m/s, lifts positively charged particles upwards. The more massive particles, which have a negative charge, settle down. The charge separation is accompanied by an increase in the electric current density up to 10^{-8}–10^{-7} A/m^2, whereas the electric charge density increases up to 10^{-9}–10^{-8} C/m^3. In this case, the electric field strength of the atmosphere dramatically increases. The value of the electric field strength could reach ~1–10 MV/m. It is known that the breakdown of clear air at the air-earth boundary occurs at a threshold electric field strength of 3 MV/m, and at an altitude of $z \approx 10$–20 km it occurs at 0.8–0.2 MV/m. In the air contaminated by the volcanic eruption materials, the value of threshold electric field strength is even lower. This means that lightning was constantly occurring in the volcanic plume, since the electric field strength exceeded the threshold. This is exactly what the results of observations show. It has been established that during the five hours of the eruption of

the Tonga volcano, about 400,000 lightning discharges were observed to occur. The highest lightning intensity took place from 05:00 to 05:15 UT. Their rate was estimated to be ~ 20,000 min^{-1}.

In the plume, the electric field strength increased by 3–5 orders of magnitude, while outside the plume it increased only by 1–2 orders of magnitude. It can be argued that the volcanic eruption led to a significant perturbation of the global electrical circuit. This, in turn, caused a number of secondary effects.

Electrical effect in the ionosphere. The processes acting in the Earth–ionosphere cavity have a characteristic time of their formation of 440 s. Therefore, electrical processes in this cavity can be considered as being quasi-stationary. Under undisturbed conditions, the ionospheric electric field strength is 0.1–1 mV/m, and the volcanic eruption leads to its increase of up to two orders of magnitude. It is important that the electric field is mapped almost without damping along the magnetic field lines into the magnetosphere, causing secondary processes in the magnetosphere and the inner radiation belt.

Note, that the maximum perturbation of the electric field is caused not directly above the volcano but shifted to the side. The displacement is associated with the influence of atmospheric winds and the transfer of the disturbance by magnetic field lines from heights of ~ 100 km to higher altitudes. The magnitude of this displacement can reach 600–800 km.

Conclusions. Theoretical studies have shown that the magnitude of the electrical effect caused by the powerful explosion of the Tonga volcano was sufficient for reliable instrumental recording.

Magnetospheric Effects That Accompanied the Explosion of the Tonga Volcano on January 15, 2022

L.F. Chernogor

V.N. Karazin Kharkiv National University, Kharkiv, Ukraine
leonid.f.chernogor@gmail.com

The purpose of this work is to theoretically assess the magnitude of the main effects in the magnetosphere caused by the powerful explosion of the Tonga volcano on January 15, 2022.

The role of electromagnetic radiation. The magnetospheric effects of the Tonga volcano are primarily associated with the intense impact of electromagnetic radiation from lightning. The vigorous electrification of the volcanic eruption products led to the fact that the number of lightning discharges reached four hundred thousand during five hours. The highest lightning intensity was observed from 05:00 UT to 05:15 UT. The rate of discharges was about twenty thousand per minute. Let us evaluate the energy of lightning. With an average energy of $\sim 10^9$ J for one lightning and an average power of $\sim 10^9$ W, we have a total energy of about 4×10^{14} J and a total power of $\sim 4\times 10^{14}$ W. Most of the energy was spent on heating and air ionization. A fraction of $\sim 10^{-4}$–10^{-3} was transformed into the energy of electromagnetic radiation. Consequently, the total energy and power of electromagnetic radiation were estimated to be $\sim 4\times 10^{10}$–4×10^{11} J and 4×10^{10}–4×10^{11} W, respectively. The radiation was concentrated within the ~10–100 kHz frequency band. Electromagnetic waves of this range effectively propagate in the Earth–ionosphere cavity and, most importantly, along magnetic field lines in ionization ducts, reaching the inner radiation belt, where they excite the cyclotron instability. In the radiation belt, electromagnetic radiation interacts with high-energy electrons (~10–100 keV), causing their partial precipitation from the magnetosphere into the ionosphere within the $z \approx 70$–120 km altitude range. In this case, the current system of the dynamo region of the ionosphere is disturbed, geomagnetic field disturbances and Alfvén waves are generated. The latter, propagating to the magnetosphere, interact with high-energy electrons of the inner radiation belt. This is how the ionosphere–magnetosphere interaction is activated.

The dynamics of electromagnetic radiation and high-energy particles in a magnetic flux tube has been studied. It has been found that a significant

part of high-energy particles can be lost from the inner radiation belt under the action of the electromagnetic radiation.

It is substantiated that the electromagnetic radiation generated due to a volcanic eruption can trigger magnetospheric processes that significantly disturb the state of the inner radiation belt.

Alfvén mechanism. The essence of this mechanism of the action in the magnetosphere is as follows. The Southern Hemisphere, where the Tonga volcano is located, unlike the Northern Hemisphere, was illuminated by the Sun. At the heights of the dynamo region, the blast wave from the volcano, having reached the ionosphere, generated a perturbation of the electron density and electric field, more precisely, an Alfvénic pulse. The latter moved with an Alfvén speed of ~300 km/s along the magnetic field line to the Northern Hemisphere, causing a disturbance in the electric field and in the downward flow of the plasma from the plasmasphere to the ionosphere. Given that the flow speed is of order of 100 m/s, the induced electric field is estimated to be 2 mV/m.

The theoretically described effects were actually observed by a number of authors. They detected a disturbance in the magnetically conjugate region over Japan. The plasma flow speed was 100–110 m/s, and $E_e \approx 2.8–3.1$ mV/m, which is in excellent agreement with our estimates.

Conclusions. The conducted theoretical studies have shown that the explosion of the powerful Tonga volcano could cause significant perturbations of the magnetosphere and the inner radiation belt.

Ionospheric Effects Accompanying the January 15, 2022 Tonga Volcano Explosion

L.F. Chernogor, Y.B. Mylovanov, V.L. Dorohov

V.N. Karazin Kharkiv National University, Kharkiv, Ukraine
leonid.f.chernogor@gmail.com

The explosion of the Tonga volcano led to significant disturbances in the ionosphere, both aperiodic and quasi-sinusoidal (wave-like). The purpose of this work is to experimentally and theoretically study the ionospheric disturbances caused by the explosion of the Tonga volcano.

Ionospheric hole. We have studied the temporal variations of the total electron content (TEC), which has been measured using the Global Navigation Satellite System. For this purpose, 42 ground stations and a number of satellites (G01, G03, G07, G08, G15, G10, G18, G23, G24, G26, G27, G29, G31, and G32) were used. The distance from the volcano to the stations varied within the 57–5,021 km range. It has been established that the TEC showed a decrease by 3–10 TECU (on average by 5 TECU) at the stations at a distance of no more than 3 Mm over the approximately 05:00–05:30 UT to 07:00–08:00 UT period. For more distant stations, the effect was weak or absent. The reduction in the TEC approximately 45 min after the explosion was called the ionospheric hole. The mechanism of the hole generation remains unknown.

Wave effects in the ionosphere. Wave processes in the atmosphere caused quasi-sinusoidal disturbances in the ionosphere. Two types of wave disturbances were observed. The largest in amplitude (up to 1.5–2 TECU) disturbances had the highest velocity (~1 km/s). Such a speed in the *F*-region of the ionosphere is characteristic of gravity waves. Most likely, they were generated by a blast wave directly above the volcano and spread in all directions from the source. The perturbation consisted of two phases. First, a compression phase, and then a rarefaction phase, again a compression phase, which was replaced by a rarefaction phase. The first disturbance was followed by the second, which had a much lower speed, amplitude, and period. The first disturbance was observed to occur with a time delay of 40 min, a duration of 80–90 min, and an amplitude of 1.3–1.6 TECU. At a distance of 2.6 Mm from the volcano, one finds a speed of ~1 km/s. The second disturbance was produced with a time delay of 125 min, a duration of 120–130 min, and an amplitude of 0.6 TECU. At a distance of 2.4 Mm,

one finds a speed of 320 m/s. From 05:30 to 07:30 UT the TEC exhibited a decrease in the trend by 3–4 TECU, which was due to the formation of the ionospheric hole. Ionospheric processes at a greater distance (3–3.2 Mm) were qualitatively similar. The hole was less pronounced, and the TEC disturbance was observed to be ~2–3 TECU. The first disturbance was directly related to the explosion of the volcano, and the second was related to the propagation of the volcano-induced atmospheric Lamb wave and to part of its energy that tunneled to ionospheric heights.

Perturbation of the ionosphere by electromagnetic radiation from lightning. On January 15, 2022, from 05:00 to 05:15 UT, the rate of lightning discharges in the volcanic plume reached 20 thousand per minute. Given a single lightning discharge power of 10^9 W and its duration of ~1 s, one has a total power of about 3×10^{11} W. A small fraction, 10^9 W, of this power is converted into electromagnetic radiation. A fraction (~10^8 W) of the latter propagates through the ionosphere along the magnetic field line into the magnetosphere. This power is enough to disturb the electron temperature and density in the ionosphere by hundreds of percent within an ~15 min interval.

The disturbance in a magnetic flux tube led to the generation of Alfven waves propagating along the magnetic field line. In addition, the plasma and heat should be slowly flown towards the magnetically conjugate region. The latter had been facilitated by a rather short length of the magnetic flux tube.

Conclusion. The explosion of the Tonga volcano caused strong aperiodic and quasi-sinusoidal disturbances in the ionosphere on a global scale.

Statistical characteristics of atmospheric waves, generated by the explosion of the Tonga volcano on January 15, 2022

L.F. Chernogor, M.B. Shevelev

V.N. Karazin Kharkiv National University, Kharkiv, Ukraine
mykyta.b.shevelev@gmail.com

General Information. The explosion of the Tonga volcano (20°32′S, 175°38′W) belongs to the unique. The height of the ejection of the eruption products reached 50–58 km. According to various data, the energy of the blast wave ranged from 4–18 to 478±191 Mt of TNT. The index of volcano explosion index (VEI) was equal to 5.8, the magnitude of the volcano was 5.5, and the intensity reached 10.8.

The explosion of the volcano generated a seismic wave (earthquake magnitude 5.8), tsunami, waves in the atmosphere and ionosphere. The atmospheric wave went around the planet 8 times. A detailed study of the parameters of atmospheric waves is an urgent task.

The purpose of this report is to determine the statistical characteristics of blast waves generated by the Tonga volcano on January 15, 2022. For the analysis, observational data obtained from the global network of barographs were used. The intensity of the blast waves was significant: at a distance of 64 km, the wave amplitude was close to 2 kPa, at a distance of 700–800 km – 0.5–0.6 kPa, and at a distance of 16–18 Mm – 0.2 kPa. According to calculations, the amplitude near the volcano was equal to hundreds of kilopascals. The duration of the blast wave was close to 50–60 minutes.

The authors built the following correlation fields and established the corresponding regression equations: the dependence of the delay time on the distance between the volcano and the observatory, the dependence of the wave arrival speed on the distance, and the dependence of the excess pressure on the distance.

Conclusions. As a result of statistical processing of observation data, the following was established.

1) The delay time of the blast wave was increased linearly with increasing distance from the volcano to the observatory.

2) The speed of propagation of the blast wave within the distance from 64 km to 136.5 Mm remained practically unchanged and amounted to 313–315 m/s. This is the speed of a Lamb wave.

3) The divergence of the blast wave front was cylindrical, which is also a property of the surface Lamb wave.

4) Depending on the trajectory of the blast wave, its orientation and the state of atmospheric weather along the path of wave propagation, the wave amplitude changed up to two times for a constant distance from the volcano to the observatory.

5) The depth of attenuation of the explosive wave was at least several hundreds of megameters, that is, it propagated practically without attenuation. This also works in favor of the Lamb wave, which was able to circle the globe up to eight times.

Analytical theory of the Doppler shift of HF radio waves along oblique propagation paths in the isotropic ionosphere

L.F. Chernogor, Y.H. Zhdanko

V.N. Karazin Kharkiv National University, Kharkiv, Ukraine
eugenezhd@gmail.com

The ionosphere is widely used as a channel for radar, radio astronomy, radio navigation, communication channels, and space-based probing the Earth. To reveal changes in the radio channel parameters and variations in dynamic ionospheric processes, measurements of the Doppler shift and signal amplitude of HF radio waves should be taken along oblique propagation paths of various orientation. The Doppler radio sounding exhibits a great sensitivity to the dynamic processes in the ionosphere, therefore, the need for further development of the theoretical basis for oblique HF radio probing the ionosphere, as a main simple and cheap technique for monitoring the ionospheric radio channel, is urgent.

The aim of this work is to develop the theoretical basis for the Doppler probing the ionosphere along oblique propagation paths and to derive simple analytical relations for the Doppler shift.

In developing the theoretical basis for oblique HF probing, the undisturbed ionosphere is assumed to be plane stratified, and the ionospheric disturbances to follow periodic and aperiodic models. The Snell's law, the general formula for the Doppler shift, and the index of refraction taken to be that for the isotropic ionosphere are involved in the analytical derivations. The main technique is calculations using an analytical approach.

Main results are as follows. The corrected secant law describing the condition for HF radio waves to reflect from a loss-free smooth spherically concentric isotropic ionosphere has been obtained. A simple analytical expression for estimating the maximum usable frequency along oblique HF propagation paths, making use of the known maximum plasma frequency, has been determined. For the conditions of oblique HF sounding the ionosphere, simple analytical relations are obtained for estimating the relative amplitude of quasi-sinusoidal disturbances and the magnitude of aperiodic disturbances of the electron density in the ionosphere. The applicability of the obtained relations has been demonstrated in practice.

Conclusions. The scientific base has been developed for making use of it in oblique HF probing the ionosphere.

Methodology and results of the study of traveling ionospheric disturbances parameters from spaced oblique HF sounding data

L.F. Chernogor, V.F. Pushin, Y.H. Zhdanko

V.N. Karazin Kharkiv National University, Kharkiv, Ukraine
eugenezhd@gmail.com

A characteristic feature of the ionospheric radio channel is that its parameters depend on season, local time, solar activity, geographic coordinates, the state of the Sun, the state of atmospheric-space weather, etc. The state of the atmosphere and ionosphere and thus the state of the corresponding radio channels is rarely quiet. Usually, they are disturbed by high-energetic sources of natural or anthropogenic nature. It is the perturbation of the parameters of the radio channel that limits the potential tactical and performance characteristics of radar, radio navigation, radio astronomy, radio communication systems, and remote radio sensing of the Earth from space. To improve the radio channel performance, the non-stationary and random disturbances need to be diagnosed, and the channel characteristics should be adapted to the disturbed conditions. The dynamic processes in the atmosphere are studied with many radio techniques, viz. ionosonde, incoherent scatter radar technique, signals from Global Positioning System satellite constellation, observations of HF radio waves at oblique incidence, etc. The oblique incidence technique can use dedicated transmitters, intercept signals from non-dedicated transmitters, utilize the transmitters of opportunity, those used for broadcasting or for dedicated

services. The technique of oblique sounding is a passive technique, and it is capable of monitoring large, up to global-scale, areas of the planet Earth. The technique shows high sensitivity since it employs measurements of the Doppler shift and the signal amplitude. Its time resolution is 10 s, and the Doppler resolution is 0.01–0.1 Hz, yielding the Doppler shift error of better than 0.01 Hz. These errors translate into the capability of monitoring electron density variations of order of 10^{-4}–10^{-3}, and vertical movement speed of 0.1–1 m/s.

The aim of this work is to present the results of determining the parameters of traveling ionospheric disturbances over the People's Republic of China by making use of the database measurements made with the multiple path oblique HF radio waves probing the ionosphere.

The multifrequency multiple path coherent system located at the Harbin Engineering University campus has been used to acquire spaced measurements along 14 oblique HF radio wave propagation paths of different lengths and orientations. Based on the harmonic model of traveling ionospheric disturbances and making use of three propagation paths, the phase shifts along two propagation paths were determined in relation to the reference path. This shift equals to the dot product of the wave vector on the known reference base, which is defined to be the vector from one transmitter to another. Generally, a superposition of traveling ionospheric disturbances with different values of wave vector and frequency occurs instead of a single traveling ionospheric disturbance. To determine the parameters of these traveling ionospheric disturbances, the cross-spectra are first calculated, which are then used for calculating the periods and phases of the cross-spectra.

The main results are as follows. Regarding spaced measurements taken along oblique HF radio wave propagation paths with the multifrequency multiple path coherent system, the technique has been developed for determining periods, horizontal wavelengths, and the azimuths of arrival of the traveling ionospheric disturbances. The cross-spectral analysis was invoked to determine the periods, horizontal wavelengths, and the azimuths of arrival of the traveling ionospheric disturbances with predominant amplitudes. The ~16–40-min period traveling ionospheric disturbances are confirmed to be generated by atmospheric gravity waves, whereas the ~10–13-min period waves are electromagnetic in nature. Usually, the relative amplitude of disturbances in the electron density was observed to be ~1–10%. As a rule, the ionospheric disturbances traveled along magnetic meridians, most often from the north to the south.

Magnetic Effects of the Unique Explosion of the Tonga Volcano

L.F. Chernogor

V.N. Karazin Kharkiv National University, Kharkiv, Ukraine
leonid.f.chernogor@gmail.com

The purpose of this work is to theoretically assess the magnetic effects caused by a powerful explosion of the Tonga volcano in the ocean, atmosphere, and the ionosphere.

The mechanisms of magnetic effects in the ocean, atmosphere, and ionosphere differ significantly. Let us consider this in more detail.

Magnetic effect in the ocean. The specific electrical conductivity of ocean water is 4 $\Omega^{-1}\cdot m^{-1}$. The oceans have streams, the speed of which usually does not exceed 1–3 m/s. The streams generate an electric field with a strength of 2×10^{-5} V/m and a current density close to 8×10^{-5} A/m^2. An estimate of a local perturbation of the magnetic field by a stream gives 10^{-7}–10^{-6} T. In the areas outside of the large streams, the water currents exhibit only fluctuations with a speed of ~ 0.1 m/s that have a scale size of ~ 1–10^2 m. In the latter case, the perturbation of the magnetic field is estimated to be ~ 0.01–1 nT, i.e., the background magnetic effect is insignificant.

The explosion of the underwater volcano generates a jet with a speed of 100–300 m/s and a diameter of 10–100 m, which increases the electrical conductivity up to 8 $\Omega^{-1}\cdot m^{-1}$, induces electric field strength, and gives rise to the electric current density, and hence to the magnitude of the local magnetic effect of up to ~ 100–3,000 nT.

The magnetic effect of the underwater explosion and volcanic eruption is very significant. However, it is practically a local effect since it belongs to quasi-magnetostatic effects. For example, the magnitude of the local magnetic effect is estimated to be 1 nT already at a distance of only 1 km.

Magnetic effect in the atmosphere. The electric field induced by the powerful volcano jet with a speed of 100–300 m/s is 2–6 mV/m. The induced current is very insignificant, its value is estimated to be $(4–12)\times10^{-17}$ A/m^2. The background value of the atmospheric current density usually is 4–5 orders of magnitude higher.

The magnetic effect in the atmosphere is associated primarily with a sharp increase in the vertical current density in the jet and plume due to the intense electrification of the explosion materials. In this case, the current density increases up to ~ 10^{-7}–10^{-6} A/m^2. Estimates of the magnetic effect

of the volcanic jet and plume in the atmosphere give a value of 0.06–0.6 nT. For a plume with a radius that reaches hundreds of kilometers, the magnitude of the magnetic effect is much larger (~ 1–10 nT).

Magnetic effect in the ionosphere. Two mechanisms may be significant for the magnetic effect in the ionosphere. The first of them is related to the perturbation of the current system in the dynamo region of the ionosphere (altitudes $z \approx 90$–130 km) by the ionospheric hole that appeared due to the volcano explosion. The second mechanism of the magnetic field disturbance is due to the generation of an external electric current in the field of atmospheric waves caused both directly by the explosion of the volcano and by the tsunami generated by the explosion. The first of the mechanisms is aperiodic, the second is quasi-periodic.

Estimates of the magnetic effect of the ionospheric hole give 0.25–2.5 nT.

The Lamb wave generated by the volcano, the gravity wave, and the wave in the atmosphere caused by the tsunami induce an external current in the ionosphere with a density of $\sim 10^{-7}$–10^{-6} A/m^2 and a magnetic effect of ~ 2.5–25 nT.

Conclusion. The magnitude of the magnetic effect of the Tonga volcano in the ocean, atmosphere, and the ionosphere is sufficient for its instrumental registration.

Comparison of ionospheric plasma drift velocity measurement results obtained at middle latitudes of the Earth's eastern and western hemispheres using incoherent scatter radar data

L.Ya. Emelyanov, S.V. Panasenko

[1]Institute of Ionosphere, Kharkiv, Ukraine
leonid.ya.emelyanov@gmail.com

We used the data acquired by the incoherent scatter radar of Institute of Ionosphere (Kharkiv, Ukraine, 49.60º N, 36.30º E, the geomagnetic latitude Φ=45.7°, longitude Λ=117.8°, the McIlwain index L=2.1) and Millstone Hill incoherent scatter radar (Massachusetts Institute of Technology, USA, 42.62° N., 71.48° W, Φ=50.76°, Λ=54.8°, L=2.54) to compare the variations in the plasma drift velocity at middle latitudes of the Earth's eastern and western hemispheres. The Millstone Hill radar data are available in the Madrigal database (http://millstonehill.haystack.mit.edu/index.html). Millstone Hill radar activity time intervals that either overlapped or were very close to those for Kharkiv radar activity were selected for analysis. For a correct use of the results from a number of experiments conducted using the Millstone Hill radar, only those data were chosen where the vertically directed antenna was involved and simple pulses with duration of 480 μs were emitted.

Millstone Hill radar data analysis was performed in such a way that the altitudes, the data accumulation time of both radars and the resolution were as close as possible to each other. To compare the temporal variations of the plasma velocity, the local time (LT) for quiet geomagnetic conditions was chosen as the time parameter. In conditions of increased geospace activity, UT time was used in addition to LT time.

Analysis of the March 21–23, 2017 data shows that the daily dependences of the plasma velocity V_z in the ionosphere over Kharkiv and Millstone Hill in spring are mostly close both qualitatively and quantitatively. The differences in the variations of V_z at night and in the morning at altitudes of 200 – 250 km are revealed. The velocity values in Kharkiv are more towards negative values by 20–50 m/s. The morning extremum of V_z (towards positive values) in Kharkiv is more pronounced compared to Millstone Hill at altitudes of 200–360 km. Conversely, the V_z evening extremum (towards negative values) in Kharkiv is less pronounced compared to Millstone Hill at altitudes of 310–470 km. ($V_z < 0$ means

downward motion of the plasma, $V_z > 0$ means upward motion). In the summer of June 20, 2019, the behavior of the V_z variations for Kharkiv and Millstone Hill is similar, but the differences are in the velocity values of about 20 m/s in the altitude range 260–360 km and more at other altitudes of ionosphere. In the winter of February 4–5 and December 15–16, 2020, the V_z variations were similar both qualitatively and quantitatively. The velocity of the downward motion of plasma in the ionosphere over Kharkiv was markedly less than over Millstone Hill only in the interval between 06:00 and 12:00 LT on February 4 and 5, at altitudes of 200–310 km.

During the geomagnetic storm on March 21–23, 2017, a correlation was noticeable between the temporal variations in the ionospheric plasma velocity over Kharkiv and Millstone Hill, mainly at altitudes of 250–420 km.

A certain difference between the measurement results of Kharkiv and Millstone Hill radars can be explained by the longitude effect. It is due to the mismatch of the geographic and geomagnetic poles, the volumes of magnetic force tubes for Kharkiv and Millstone Hill differ significantly (2.14 times). The latitude positions of the magnetically conjugate regions in the Earth's southern hemisphere for Kharkiv and Millstone Hill also differ significantly, and, as a consequence, the exchange processes between the ionosphere and the protonosphere can differ. That is why the simultaneous coordinated measurements of the ionospheric plasma velocity (together with other ionospheric parameters) carried out by the Kharkiv and Millstone Hill radars are very important for the study of effects in the ionosphere.

Heat waves over Ukraine detected by HCWI

A.O. Kornus[1,2], S.V. Klok[3], O.H. Kornus[1], O.S. Danylchenko[1]

[1]Sumy A.S. Makarenko State Pedagogical University, Sumy, Ukraine
[2]Sumy State University, Sumy, Ukraine
[3]Ukrainian Hydro Meteorological Institute, Kyiv, Ukraine
a_kornus@ukr.net

Heat and Cold Wave Index (HCWI) is implemented in the Copernicus European Drought Observatory (EDO). HCWI is used to detect and monitor periods of extreme-temperature anomalies (i.e. heat waves) that can have strong impacts on human activities and health. This is one of the climate indexes that takes into account both HW duration and intensity. The HCWI indicator is computed for each location (grid cell), using the methodology developed by Lavaysse et al. (2018), and based on the JRC's MARS AGRI4CAST database of daily meteorological observations. In accordance with EDO, HW defined as events of at least three consecutive "hot" days. In this context, a "hot day" is a day with both daily air minimum and maximum temperatures (Tmin and Tmax) are above their daily threshold values, calculated as the 90th percentile values of Tmin and Tmax for that calendar day during the 30-year climatological baseline period (1981-2010).

As a result of analysis of the series of daily air temperature for 1980-2021 there are 83 HW events that met the criteria for defining this event, which is used in this study, were recorded in Ukraine (on the average 2 events per year). At the same time, the uneven manifestation of this atmospheric phenomenon in time is clearly traced with the allocation of two half-periods, the duration of which is 21 years. For the first half-period (1980-2000) 29 events of HW were recorded, and for second half-period (2001-2021) − already 54 events. It should be noted that 1-2 events of HWs were usually recorded in Ukraine per year until 2001, but in the second half-period their frequency increased to 2-3 events, and in some years reached to 4-5 events per year.

According to the EDO methodology, the minimum duration for which the HW is recorded is 3 days. The maximum length of HW over Ukraine for the study period 1980-2021 ranged from 4 (1984) to 20 (2010 and 2013) days. So, the average duration is 4.2 days, and the average maximum length of HW is 9.45 days. The results of the study show that all indicators characterizing the duration of HW increased during study period. If for

1980-2000 the average duration of heat waves was 3.8 days, then for 2001-2021 the average duration increased to 4.3 days. The average maximum length of HW increased more significantly − from 7.4 to 11.5 days in the second half-period.

To characterize the intensity of HW, as a rule, the cumulative T_{max} during a single HW is used. J. Kyselý (2010) notes that this characteristic is the most convenient for wave intensity evaluation. Usually, the cumulative T_{max} during an individual HW is calculated as the sum of the differences between the maximum daily air temperature and a certain limit value, depending on the HW definition. However, such an indicator can also be the temperature of hottest day of the HW event. It was used in a recent work about Ukraine (Shevchenko et al., 2020). The intensity of the HW determined according EDO as the maximum air temperature extreme. Over Ukraine, the hottest HW events for the study period were with a maximum daily temperature of 41.4 °C (2010), and mean (1980-2021) temperature extreme of the HW over Ukraine is 32.2 °C.

The “coolest” HWs were in 1980, 1982, 1984 and 1990, and the hottest HW were in 2022, 2007 2010 and 2017, when the temperature extreme exceeded 40 °C. That was expected that the hottest waves are in the south of Ukraine, where the temperature extreme reached 45.8 °C (1999) and 46.8 °C (2021).

Change in particle fluxes in Earth magnetosphere during substorm events

L. Kozak[1,2], E. Kronberg[3], B. Petrenko[1,2], R. Akhmetshyn[1], I. Ballai[4]

[1]Taras Shevchenko National University of Kyiv, Ukraine
[2]Space Research Institute of the National Academy of Sciences of Ukraine and the State Space Academy of Ukraine, Kyiv, Ukraine
[3]Geophysics Department of Earth and Environmental Sciences University of Munich, Munich, Germany
[4]School of Mathematics & Statistics at The University of Sheffield, UK
gutovska@ukr.net, roman_akhmetshyn@univ.kiev.ua

The source of ions in the magnetosphere can be both the solar wind and the ionosphere. How active do ions fill the magnetosphere depends on the level of geomagnetic activity, heating of solar wind ions at the front of the shock wave, modulation in the area of magnetic line reconnection, etc.

The presence of heavy ions at an altitude of the magnetosphere will significantly change the physics of the processes taking place there. That is because in addition to the change in main characteristics of the plasma (pressure, Alfvén velocity, thickness of the current/plasma layer), the conditions and rate of development of instabilities (in particular Kelvin-Helmholtz instabilities) will also change.

The paper demonstrates the change in fluxes and wave-particle interaction during a substorm for a separate event (September 11, 2014) and presents a statistical review of the change in particle fluxes in the region of magnetic field depolarization for 2001-2015 using the method of superposed epochs. Magnetic field measurements from ferrosonde magnetometers (FGM) and high-energy proton flux values from RAPID spectrometer measurements in the energy range of 20–400 keV were used for the analysis. During the substorm, a selective non-adiabatic acceleration of some of the protons that depends on their energy (decrease in the flux of low-energy protons and increase in high-energy protons), and an increase in the power of magnetic field fluctuations at the gyro-frequencies of heavy ions (helium and oxygen) were recorded.

This work was supported by the grant no. 97742 of the Volkswagen Foundation (VW-Stiftung), the Royal Society International Exchanges Scheme 2021 IES\R1\211177, and BF/30-2021.

Infrasound observations at Vernadsky Station of the January 2022 Hunga eruption, Tonga

O.I. Liashchuk[1], Yu.A. Andrushchenko[1], Yu.S. Otruba[2]

[1]Main Center of Special Monitoring, Gorodok, Ukraine
[2]National Antarctic Scientific Center, Kyiv, Ukraine
alex_liashchuk@ukr.net

On January 15, 2022, the eruption of Hunga volcano, Tonga, caused an incredibly powerful explosion in the atmosphere, which had never before been recorded by measuring networks. The event was recorded at the Ukrainian Antarctic Station "Akademik Vernadsky" by the geophysical complex in the form of acoustic waves and tsunami waves at a distance of 8870 km.

The UAS infrasound station is an array of four sensors with a 100 m aperture. All sensors are equipped with primitive wind noise suppression systems to reduce small-scale interference on the sensor. Infrasound monitoring capabilities are limited by aperture and local wind conditions, especially those associated with atmospheric convective turbulence. The installed sensors are microbarometers sensitive to pressure changes up to 720 Pa. The station continuously measures differential pressure at a frequency of 40 Hz. The instrumental characteristic of this channel is designed for the frequency range ~0.05–10 Hz.

To process infrasound records and characterize the coherent properties of the wavefront, the progressive multichannel correlation method (PMCC) is applied to the infrasound array data. This method, implemented in the PMCC software, estimates arrival parameters based on inter-element cross-correlation and time delays.

The results of data processing show that the speed of propagation of the acoustic wave was 316 m/s, the speed of propagation of infrasound was 328 m/s. The true azimuth to the source is 242.18 degrees, the calculation according to the data of the infrasound group showed 240.5 degrees. The second acoustic wave arrived at Vernadsky station at 16:05. The infrasound azimuth differs from the initial one by 5 degrees, which may be due to the passage of the wave through the circumpolar vortex.

The magnitude of the atmospheric pressure surge was 170 Pa, the infrasound amplitude averaged over four channels was 18 Pa. A tsunami wave was recorded also with maximum amplitude of 32 cm.

Coordinated study and comparative analysis of ionospheric processes over Ukraine and Japan using radar, satellite and model data

S.V. Panasenko[1], D.V. Kotov[1], Y. Otsuka[2], M. Yamamoto[3], H. Hashiguchi[3], O.V. Bogomaz[1], M.O. Reznychenko[1]

[1]Institute of ionosphere, Kharkiv, Ukraine;
[2]Institute for Space-Earth Environmental Research, Nagoya University, Nagoya, Japan
[3]Research Institute for Sustainable Humanosphere, Kyoto University, Uji, Japan
sergii.v.panasenko@gmail.com

Characteristics of geospace environment all over the world are greatly important for studying to understand and predict space weather phenomena occurring during different solar and magnetic activity conditions. Strong space weather events are known to cause significant variations in ionosphere and atmosphere parameters and can result in a damage of power infrastructure and its space-based assets. Evidences of even weak space weather changes were detected to affect the ionospheric and plasmaspheric plasma processes. Satellite and radar observations provide reliable information about the ionospheric processes, but they yield the data having the sparseness in temporal and/or spatial domain that precludes monitoring all the time and over all locations. Various models can reproduce the temporal variations of ionospheric and atmospheric parameters over definite location but they may incorrectly reflect realty due to the lack of the experimental data on which empirical models are based or incomplete knowledge about input or embedded parameter values used for theoretical models. The best way to reduce these differences is to use data assimilation models which account for diurnal and/or regional features or are constrained to follow the observed variations.

In the current study, we performed a comparative analysis of results from ground- and satellite-based observations jointly conducted over Ukraine and Japan as well as from ionospheric and plasmaspheric model simulations for both regions. The aim of this study is twofold. First, we focused on study and analysis of new experimental results, which display the longitudinal difference and enable improving the regional and global ionospheric models. Second, this research was intended to validate models and facilities over two regions during specific conditions near solar

minimum. The Kharkiv incoherent scatter and Shigaraki MU radars, the Swarm and DMSP satellites, International Reference Ionosphere (IRI-2016) empirical model, and Field Line Interhemispheric Plasma (FLIP) physical model were employed to detect regular variations of such the main plasma parameters at the F2-layer peak and in the topside ionosphere as electron density, electron and ion temperatures, as well as traveling ionospheric disturbances (TIDs) over both regions.

Coordinated observational campaign conducted during 5 – 6 September of 2017 and completed by appropriate model simulations provided the following key results. Regular variations of the main plasma parameters at the F2-layer peak and in the topside ionosphere are close for Kharkiv (Ukraine) and Shigaraki (Japan) qualitatively and quantitatively. IRI empirical model is capable to predict the key qualitative features of variations in ionospheric plasma parameters over Kharkiv and Shigaraki. However, the predictions still need to be improved quantitatively. Any of the optional IRI sub-models of F2-layer peak height, topside electron density, and temperature cannot be considered as preferable. FLIP physical model provides the best agreement with the observations being constrained to follow the observed diurnal variations of F2-layer peak height. For the first time, the need to increase neutral hydrogen density in NRLMSISE-00 model by at least a factor of 2 was established in Asian longitudinal sector. The same need is seen also for European sector. TIDs induced by solar terminator passages were detected both over Kharkiv and Shigaraki. They exhibit the different dominant periods of about 50 min and 80 min over Europe and Japan, respectively. This could reflect the regional features, in particular, the difference in latitudes, longitudes, and magnetic inclination/declination and need to be further investigated.

Long-term and short-term aerosol observations in the atmosphere over Kyiv with the AERONET sun-photometers

Yu. Yukhymchuk[1,2,3], V. Danylevsky[1,4], G. Milinevsky[1,4,5]

[1]Main Astronomical Observatory of National Academy of Sciences of Ukraine, Kyiv, Ukraine
[2]Laboratoire d'Optique Atmosphérique, University of Lille, Lille, France
[3]Institute of Physics of National Academy of Sciences of Ukraine, Kyiv, Ukraine
[4]Taras Shevchenko National University of Kyiv, Kyiv, Ukraine
[5]College of Physics, International Center of Future Science, Jilin University, Changchun, China
yuliia.yukhymchuk@mao.kiev.ua

The AERONET (AErosol RObotic NETwork) is one of the most advanced remote sensing aerosol monitoring systems. This network is operated by NASA (USA) and the French and Spanish ACTRIS (Aerosols Clouds and TRace gas InfraStructure) components in Europe. At the moment, it includes several hundred working stations around the globe. The Kyiv station is located on the roof of the Main Astronomical Observatory in the capital of Ukraine. It is equipped with CIMEL CE318 sun photometers and has been provided observations since 2008. The tools of AERONET allowed obtaining long-term series of proper aerosol parameters such as Aerosol Optical Depth (AOD), and Angstrom Exponent (AE). Long-term observations (from 2008 until now) of AOD, AE, and radiative forcing are presented in this work. These data can be used to analyze the aerosol particle variations, studying the seasonal dynamics and the local aerosol behavior. In addition, some period of the simultaneous measurements of two sun-photometers at the same station is also analyzed (Figure 1).

Figure 1. Simultaneous observations of two CIMEL sun-photometers for intercalibration.

The automatic observations by CIMEL CE318 sun-photometer provide the possibility to study aerosol amount and properties data collection in the condition of full-scale russian aggression. This information allows estimating the impact of war on air contamination to the atmosphere over Kyiv.

This work was partly supported by Space Program for 2018-2022 of the National Academy of Sciences of Ukraine through the project 03/22 and from the European Union's Horizon 2020 research and innovation program under the Marie Skłodowska-Curie grant agreement No 778349 GRASP-ACE and research and innovation program under ACTRIS-2 grant agreement No 654109. We thank Brent Holben (NASA/GSFC) for managing the AERONET program.

Modelling the excitation of coupled Schumann-Alfven resonator. Penetration of electric field into the ionosphere and problem of dynamic-quasistatic limiting pass

Yu. Rapoport[1,2,3], V. Grimalsky[4], A. Krankowski[1], K. Kacper[1], S. Petrishchevskii[2], A. Grytsai[2], A. Liashchuk[3], A. De Santis[5], C. Scotto[5]

[1]University of Warmia and Mazury in Olsztyn, Poland
[2]Taras Shevchenko National University of Kyiv, Kyiv, Ukraine
[3]National Center for Control and Testing of Space Facilities of the State Space Agency of Ukraine (NCCSSAU)
[4]University of State Morelos (UAEM), Cuernavaca, Mexico
[5] Istituto Nazionale di Geofisica e Vulcanologia (INGV), Italy
msergiyp@gmail.com

The Ionospheric Schumann and Ionospheric Alfven resonators and the waveguide Earth-Ionosphere (WGEI) are excited in ultra-low frequency (ULF) and very low frequency (VLF) ranges respectively. We consider theory of excitation both Schumann resonator and Alfven resonator for ULF electromagnetic oscillations by powerful sources in the lower atmosphere. Corresponding calculations shown that an excitation of ULF oscillation in coupled Schumann Resonator - Ionospheric Alfven Resonator with relatively large, for geophysical wave processes, quality factor (> 10) are possible. These results can be important for the understanding of the ionospheric response to the powerful eruption of the Hunga-Tonga volcano (January 2022).

Concerning the propagation of electromagnetic waves (EMWs) of VLF range in WGEI, it was shown that at a distance of about 1000 km from the sources only the lower few ones VLF modes remain noticeable.

There is a problem of limiting pass from dynamic to quasi-stationary determination of the electric field penetrating to the upper ionosphere and magnetosphere, when the frequency of the current source, located in the lower atmosphere, decreases. Model of penetration of ULF electric field through the Lithosphere (Earth)-Atmosphere-Ionosphere-Magnetosphere (LEAIM) system with given sources in the lover atmosphere is developed. The solution of the problem of limiting pass from dynamic to quasistatic modelling including quasimagnetostatic field is proposed.

Remotely visible atmospheric NO_2 changes in Ukraine due to the Ukrainian-Russian war using TROPOMI data

M. Savenets

Ukrainian Hydrometeorological Institute, Kyiv, Ukraine
savenetsm@gmail.com

The Russian full-scale invasion on February 24th, 2022, caused unprecedented environmental changes in Ukraine. Atmospheric air quality faced the influence of new "war-originated" emission sources and significant changes in usual anthropogenic activities. This study presents the picture of air pollution changes, which is well detected using TROPOspheric Monitoring Instrument (TROPOMI) data onboard the Sentinel-5 Precursor satellite. The results are focused on nitrogen dioxide (NO_2) tropospheric column data that is usually considered as the best indicator of air quality based on remote sensing measurements. In order to consider the background NO_2 changes, ERA5 meteorological data was used to estimate the impact of weather conditions on the possibility of accumulating and dispersing atmospheric pollutants.

Overall, NO_2 content decreased over urban areas by up to -2.0^{-5} mol/m^2 as a result of the shutdown of industrial facilities (temporary stoppage or full destruction). The huge role in northern, eastern, and southern cities played a significant decrease in traffic activity on the streets. However, NO_2 content increased by up to 1.0^{-5} mol/m^2 along the entire contact line because of frequent wildfires after shelling. Numerous high-content NO_2 were detected in areas far from industrial regions and big cities, which were not associated with wildfires and were only observed for a single sounding time. These spots might correspond to the fuel emissions from military equipment. In February and March 2022, intense NO_2 emissions were detected on Russian territory near the Ukrainian border, indicating the role of military activity in the region. Starting from May 2022, the influence of war had mostly localized effects. The most typical among them were pollutants' emissions from numerous wildfires, less pollutant urban emissions (but the features of spatio-temporal distribution were rather specific depending on the city), and short-term NO_2 content maxima as a consequence of explosions after missile attacks.

Polarimetry of stratospheric aerosol

M. Sosonkin[1], I. Syniavskyi[1], J. Dlugach[1], Yu. Ivanov[1], Ye. Oberemok[2], G. Milinevsky[1,2,3], V. Danylevsky[2]

[1]Main Astronomical Observatory, National Academy of Sciences of Ukraine, Kyiv, Ukraine
[2]Taras Shevchenko National University of Kyiv, Kyiv, Ukraine
[3]College of Physics, International Center of Future Science, Jilin University, Changchun, China
msosonkin@gmail.com

The stratospheric aerosol layer impacts short-term and long-term changes in the energy balance of the entire Earth atmosphere. The composition and amount of aerosol particles in stratosphere are changed significantly due to unpredictable volcanic eruptions. In addition, the idea of aerosol artificial injection in the stratosphere is gaining increasingly practical content. Geoengineering propose release aerosol into the stratosphere in an amount that can reduce significantly the solar radiation at the Earth surface. This requires a comprehensive model to study the processes and possible consequences on the basis of well-balanced experimental data. Measurements from the spacecraft are effective part of these studies.

Polarimetric measurements of scattered radiation are a powerful tool for determining the microphysical parameters of aerosol, but the use of this method to study the stratosphere aerosol layer from the orbit is limited by small aerosol optical thickness in comparison to the background complex distribution of brightness of the underlying surface. Morozhenko et al. (2014) proposed to provide the remote measurements of the stratosphere aerosol properties in the UV spectral band $\lambda < 300$ nm of the Earth's atmosphere "opacity", which shades the surface of the Earth. Choosing a water vapor absorption band in the atmosphere 1.378 μm is much more acceptable. Model computations performed in Mishchenko et al. (2019) and Dlugach et al. (2021) showed that precise multi-angle photopolarimetric measurements in a 1.378-мм spectral channel would enable reliable retrievals of microphysical characteristics of stratospheric aerosols. Reliable microphysical characteristics can be obtained both during the powerful volcanic eruption and the "background" state of the stratosphere.

With joint efforts of the Main Astronomical Observatory NAS of Ukraine and Taras Shevchenko National University of Kyiv, the complex of scientific equipment for studying the stratospheric aerosol layer on the satellite in the Cubesat 3x2U format are developing (Figure 1).

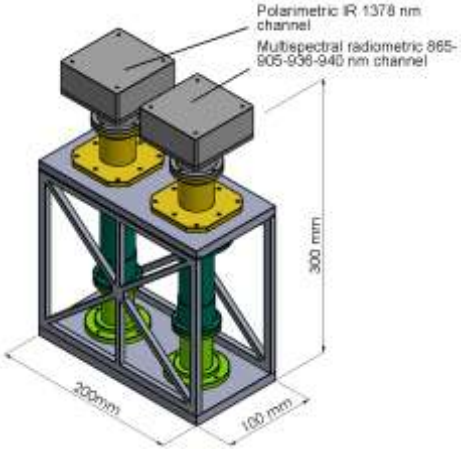

Figure 1. NIR-imaging polarimeter in Cubesat 3x2U format

The NIR-imaging polarimeter consists of two optical channels using the scheme with the separation of the input pupil of the existing polarimetric channel from the multispectral imaging polarimeter MSIP, which is adjusted for a wavelength of 1.378 μm with slight changes. The quality of the planned measurements, among other things, should be ensured by constant monitoring of the amount of water vapor in the atmosphere. For this purpose, the payload will provide a radiometric channel of the MSIP with wavelengths 865, 905, 936 and 940 nm to determine the water vapor by the protocol used by MODIS.

This work was partly supported by Space Program for 2018-2022 of the National Academy of Sciences of Ukraine through the project 03/22, Ukraine; by Ministry of Education and Science of Ukraine, Kyiv, through the projects 20BF051-02 and BF30-2021; by College of Physics International Center of Future Science, Jilin University, China. This work also was partly supported from the European Union's Horizon 2020 research and innovation program under the Marie Skłodowska-Curie grant agreement No 778349 GRASP-ACE.

Morozhenko, A.V., Vidmachenko, A.P., Nevodovskiy, P.V., Kostogryz N.M. On the efficiency of polarization measurements while studying aerosols in the terrestrial atmosphere. Kinemat. Phys. Celest. Bodies, 2014, 30, 11–21. https://doi.org/10.3103/S0884591314010061.

Mishchenko, M.I., Dlugach, J.M., Lacis, A.A., Travis, L.D., Cairns, B. Retrieval of volcanic and man-made stratospheric aerosols from orbital polarimetric measurements. Opt. Express, 2019, 27, A158–A170. https:// doi.org/ 10.1364/OE.27.00A158.

Dlugach, J.M., Mishchenko, M.I., Veles, O.A. Applying orbital multi-angle photopolarimetric observations to study properties of aerosols in the Earth's atmosphere: Implications of measurements in the 1.378-μm spectral channel to retrieve microphysical characteristics and composition of stratospheric aerosols. *J. Quant. Spectrosc. Radiat. Transfer,* 2021, 261, 107483-107502, doi:10.1016/j.jqsrt.2020.107483.

Manifestation of weekly cyclicity and dynamics in some parameters of the atmosphere according to data from the AERONET station in the Martova

A.V. Soina

Institute of Radio Astronomy of the National Academy of Sciences of Ukraine, Kharkiv, Ukraine
adituanna@gmail.com

From December 2013 to December 2019, an AERONET global network point with coordinates 50.364 N, 36,953 E worked in the village of Martova in Kharkiv Oblast, on the basis of the Low-Frequency Observatory (LFO) of the National Academy of Sciences of Ukraine. This network is based on the operation of automatic unified sun photometers Cimel CE-318 (France), designed to fix diffuse and direct solar radiation at several wavelengths from 340 to 1640 nm. Among the three levels of data, we used Level 2.0 data, which is the most accurate. In the village Martova, photometer was installed in a recreational area at a considerable distance from large cities and industrial sources of environmental pollution (more than 50 km from the city of Kharkiv), on the shore of the Pecheneg reservoir.

Previously, we investigated weekly variations in this monitoring point and in Kyiv, and also searched for the manifestation of the weekend effect

on a global scale and in the largest industrially developed regions of the planet. The similarity of the behavior of the weekend effect was established. So far, a seven-day cyclical search was conducted according to the seasons of the year in the village Martova, and also analyzed the dynamics of changes in AOT870, AOT440, precipitated water and the Angstrom parameter during the period when the photometer was operating at the LFO. The work shows the graphs of the dynamics of the specified parameters and the maximum and minimum values for the month.

Based on the results of the study, it was established that: (1) at the level of AOT440 and AOT870, the phenomenon of the weekend effect manifests itself best in the summer. In winter it is associated with local influence, in spring it is absent, and in autumn its maximum shifts from Thursday (summer) to Tuesday-Wednesday; (2) in the amount of deposited water, a weekly cycle is observed in the autumn period - it is well defined with the maximum value on Wednesday and the minimum value on Friday and on weekends; (3) in the Angstrom parameter, one can note a clear manifestation of seven-day variations in winter; (4) the highest indicators of AOT870 and AOT440 are observed in 2017 and 2018, respectively, and in the amount of deposited water and Angstrom parameter in 2018 and 2016, respectively.

Next, we plan to provide correlation analysis of the data obtained in Martova and Kyiv AERONET stations.

We thank Brent Holben (NASA/GSFC) for managing the AERONET program and two supervisors of the AERONET Martova station for providing the sun-photometer operation.

Rossby wave characteristics in the Arctic from satellite measurements

A. Grytsai[1], G. Milinevsky[1,2,3], A. Klekociuk[4,5], O. Ivaniha[1,3]

[1]Physics Faculty, Taras Shevchenko National University of Kyiv, Ukraine
[2]College of Physics, International Center of Future Science, Jilin University, Changchun, China
[3]Department of Atmosphere Physics and Geospace, National Antarctic Scientific Center, Kyiv, Ukraine
[4]Antarctic Climate Program, Australian Antarctic Division, Kingston, Australia
[5]Department of Physics, University of Adelaide, Adelaide 5005, Australia
a.grytsai@gmail.com

We have analyzed TOMS (2000–2004) and OMI (2005–2021) total ozone column (TOC) data in January–March in the moderate and high latitudes of the Northern Hemisphere (50–80°N). Choice of this time and latitude range is caused by significant disturbances of the stratosphere parameters by Rossby waves including sudden stratospheric warming events. Our goal is to characterize variations in both TOC and Rossby wave parameters. Characteristics of the Fourier harmonics with wave zonal numbers 1–5 are studied. In particular, linear trends in the amplitudes of the prevailing quasi-stationary wave 1 are estimated.

We have indicated distinctions in behavior of the wave-1 amplitude in winters with sudden stratospheric warming and without them. It is important that amplitude of the quasi-stationary wave-1 is determined by tropospheric pressure anomalies, predominantly the Aleutian Low (TOC zonal maximum) and the North Atlantic – European High (TOC zonal minimum). The wave amplitudes and TOC interannual variations are largest in the polar cap. The positive TOC peaks were observed inside the vortex in 2010 and 2018 alternating with negative deviations in 2011 and 2020. It is shown that the Arctic Oscillation negatively correlates with TOC exhibiting Pearson correlation coefficient –0.56 at 70°N. Polar vortex strengthening and cooling are associated with positive Arctic Oscillation, which is accompanied by negative ozone deviations. Our study confirms the dominant role of zonal wave-1 (mainly, due to its quasi-stationary

component) in the winter Arctic ozone distribution. Variations in the wave-1 amplitude and phase under strong vortex conditions in 2020 and weak vortex in 2021 have been studied. A negative trend of the quasi-stationary wave-1 in middle latitude was revealed with the value –4.8 Dobson Units per decade at 50°N.

This work was partly supported by Ministry of Education and Science of Ukraine, Kyiv, through the projects 20BF051-02 and BF30-2021; by College of Physics International Center of Future Science, Jilin University, China, and by National Antarctic Scientific Center of Ukraine.

The first results of microwave radiometer CO and O3 profile measurements in the atmosphere over the northeast region of China

Y. Shi[1], V. Shulga[1,2], P. Forkman[3], W. Han[1], H. Liu[1], A. Pilipenko[1], X. Wang[1], G. Milinevsky[1,4], D. Shulga[1], O. Antyufeyev[1], D. Chechotkin[1], O. Korolev[1], V. Myshenko[1], K. Marenko[1]

[1]College of Physics, International Center of Future Science, Jilin University, Changchun, China
[2]Institute of Radio Astronomy, NAS of Ukraine, Kharkiv, Ukraine
[3]Department of Earth and Space Sciences, Chalmers University of Technology, Gothenburg, Sweden
[4]Physics Faculty, Taras Shevchenko National University of Kyiv, Ukraine
shiyu18@mails.jlu.edu.cn

The preliminary results of microwave radiometer CO and O3 profile measurements in the atmosphere over the northeast region of China are presented. We discuss the maintenance and data processing for recently installed in Jilin University the groundbased millimeter-wave radiometer for monitoring of the small atmospheric constitutes and the wind in upper stratosphere and mesosphere. This new groundbased 110–115 GHz microwave radiometer (MWR) can provide ozone O_3 and carbon monoxide CO vertical profiles in the atmosphere with the altitude coverage of 20–100 km. The retrieval algorithm used for measurements processing includes a forward model line–by–line radiative transfer calculation and an inversion to estimate of the atmospheric parameters. The radiometer parameters and peculiarities, calibration scheme, and observation method are presented. The retrieval procedure, including compensation of the different

tropospheric attenuations at the two frequencies and error characterization, also shortly described. The radiometer is currently providing vertical profiles to altitudes of the mesopause region during day and night.

The first results of the MWR measurements in Changchun show the consistency in retrieved altitude O_3 and CO profiles with satellite measurements. We analyzed the average kernel matrix and measured response for O3 and CO. The vertical confident interval of ozone molecular inversion is about 25–62 km, and the vertical confident interval of CO molecular is about 65–95 km. To use the MWR radiometer for wind data measurements we need to improve retrieval algorithm and provide mechanical works to allow observations in two directions quasi-simultaneously.

This work was partly supported by College of Physics, International Center of Future Science, Jilin University, China and by Ministry of Education and Science of Ukraine, Kyiv, through the projects 20BF051-02 and BF30-2021.

On indicators for possible forecast the development of sudden stratosphere warming

O. Ivaniha[1,2], G. Milinevsky[1,2,3], O. Evtushevsky[2], Yu. Andrienko[2], Y. Shi[3], A. Grytsai[2]

[1]National Antarctic Scientific Center, Kyiv, Ukraine
[2]Physics Faculty, Taras Shevchenko National University of Kyiv, Ukraine
[3]College of Physics, International Center of Future Science, Jilin University, Changchun, China
ivaoksi94@gmail.com

One of the key parameters affecting the appearance and intensity of sudden stratospheric warming (SSW) is the strength and characteristics of the polar vortex in winter. The strength of the polar vortex and the activity of planetary waves during the SSW can effect on the characteristics of this event. The activity of the quasi-stationary waves in the lower stratosphere during the autumn for the Northern Hemisphere and winter of the Southern Hemisphere may indicate the probable state and dynamics of the polar vortex of the corresponding hemisphere in the following months. As shown in our recent papers the amplitude of the stratospheric quasi-stationary waves in August serves as a key indicator as a level of dynamic perturbation

of the polar vortex in the spring and the possible time of the seasonal final disappearance of the ozone hole.

Traveling planetary waves that propagate upward also have a very strong impact on the dynamics and development of the SSW. They are generated by various phenomena in the atmosphere, which are described by different modes, and then propagate from the tropical troposphere to the polar stratosphere. These climate modes are El-Nino Oscillation, Quasi-Biennial Oscillation, Madden-Julian Oscillation, and Arctic Oscillation. They strongly modify the state of the polar vortex and can either encourage the occurrence of sudden stratospheric warming or inhibit it. We search possible indicators between these modes that can help in prediction the SSW appearance and behavior.

It is known that short-term forecasts give sufficiently reliable data on the development of stratosphere processes on a synoptic scale on 5-10 days. On seasonal scale existing forecasts are less reliable and can only determine the general trends of atmospheric conditions. Our analysis of stratospheric quasi-stationary waves and indices of the ocean surface temperature allowed realistically predict the development of anomalous ozone holes in 2017 and 2019 with quite accurate quantitative estimates (Milinevsky et al., 2020).

This work was partly supported by the projects 20BF051-02 and BF/30-2021 Taras Shevchenko National University of Kyiv. Part of this research was performed at the International Center of Future Science, Jilin University (JLU), under the contract with the JLU.

Milinevsky G., Evtushevsky O., Klekociuk A., Wang Y., Grytsai A., Shulga V., Ivaniha O. Early indications of anomalous behavior in the 2019 spring ozone hole over Antarctica. Intern. J. Remote Sens., 2020. 41(19), 7530–7540. https://doi.org/10.1080/2150704X.2020.1763497

Astronomical optical instrument making in the Main Astronomical Observatory National Academy of Sciences of Ukraine

I. Syniavskyi, Yu. Ivanov

Main Astronomical Observatory, National Academy of Sciences of Ukraine, Kyiv, Ukraine
syn@mao.kiev.ua

The Main Astronomical Observatory of the National Academy of Sciences of Ukraine is a well-known world-class scientific institution that develops astronomical instruments for the study of celestial objects, both for ground-based telescopes and for space-based devices. The world's best camera lens for the study of the Earth's atmosphere (aurora borealis) has been developed. An extremely large geometric factor allows the camera to operate in hyperspectral shooting mode.

The echelle spectrometer of the mid-IR range of the international ExoMars mission has been developed for the study of the vertical distribution of the mixture of small components in the atmosphere of Mars, the search for possible sources of outflows, the determination of isotopic relationships and their variations.

As part of the European project "Burst Optical Observer and Transient Exploring System (BOOTES)", the four-channel Stokes polarimeter for polarimetry of fast-moving gamma-ray bursts using large telescopes was developed and assembled. A series of Stokes polarimeter has been developed for small telescopes for astronomical observations of stars and extended objects.

Experimental samples of scanning polarimeter ScanPol and multispectral imaging polarimeter MSIP of the future Aerosol-UA space experiment were developed.

The design and development of devices includes the following stages:

– analysis of initial technical conditions, dimensional and aberration calculation of optical systems used in modern programs for design of optical systems (Zemax, Code V);

– signal/noise estimation;

– modeling of the instrument design using CAD programs (SolidWorks, AutoCad, Autodesk Inventor);

– Error budget estimation of the elements manufacture and subsystem assembly (Zemax);

– temperature range estimation, analysis of image quality (Zemax, SolidWorks, ANSYS);

– assembly, adjustment and quality control of instruments, using measuring equipment – collimators, flat mirrors, goniometers, targets; optical device assembly is carried out in clean rooms, cleanliness class ISO 6.

This work was partly supported by Space Program for 2018-2022 of the National Academy of Sciences of Ukraine through the project 03/22.

Comparison of in-situ aerosol measurement results by EcoCity and SDL607 sensors

A.O. Simon[1,2], M.M. Reshetnyk[2], G.P. Milinevsky[2,3]

[1]National Center of Junior Academy of Sciences of Ukraine, Kyiv, Ukraine
[2]Physics Faculty, Taras Shevchenko National University of Kyiv, Kyiv, Ukraine
[3]College of Physics, International Center of Future Science, Jilin University, Changchun, China
andrii.o.simon@gmail.com

In order to control air quality, we have installed two different types of aerosol in-situ sensors at the level of the 4th floor of the laboratory building of the Physics Faculty, Taras Shevchenko National University of Kyiv. The sensors are located at a significant distance from the main roads, so the results should be smoothed from short-time varied emissions from cars associated with their irregular traffic.

Comparison of the data obtained from both sensors shows a good correlation of PM2.5 and PM10 values. The EcoCity sensor is built on the *Arduino* hardware. It allows measuring the relative humidity, temperature and air pressure. However, one of the disadvantages of this sensor is the periodic gaps for measuring aerosols, while the atmospheric parameters continue to be recorded. After the correlation, this makes possible to extrapolate the atmosphere (humidity and air pressure) from the EcoCity sensor to the SDL607 data sensor, which is more reliable and intercalibrated with AirVisual sensors (Zhang et al. 2022).

The results of 2020-2021 data by the SDL607 sensor measurements and the seasonal variations of the average daily PM2.5 and PM10 values were investigated and discussed. In the winter season and in the spring and

autumn months, the amount of aerosols significantly exceeds the summer values.

This work was partly supported by Ministry of Education and Science of Ukraine, Kyiv, through the projects 20BF051-02 and BF30-2021.

Zhang, C., Shulga, V., Milinevsky, G., Danylevsky, V., Yukhymchuk, Y., et al. Spring 2020 Atmospheric Aerosol Contamination over Kyiv City. Atmosphere, 2022, 13(5), 687. https://doi.org/10.3390/atmos13050687.

ІСТОРІЯ АСТРОНОМІЇ

HISTORY OF ASTRONOMY

V.P. Tsesevich (11.10.1907-28.10.1983) and his scientific school on variable stars

I.L. Andronov

Odesa National Maritime University, Odesa, Ukraine

Volodymyr Platonovych Tsesevich was a great scientist, lecturer, organizer of science and a popularizer. His father Platon Ivanovych was a famous opera singer in Kiev (bass voice), mother - Kuznetsova Elisaveta Oleksandrivna, an opera actress, later pedagogue. Exactly 100 years ago, in 1922, at the age of 15, V.P. Tsesevich started his studies in the University, as well as observations of variable stars. Totally, he authored a huge number of ~760 publications (monographs (22), scientific and popular papers, interviews). He was a supervisor of 41 PhDs, many of them later became Doctors of Science and Professors and worked in different astronomical organizations in different cities and countries. He was a "Director of 3 observatories": where his contribution for the development was great. In 1933-1937, he worked as a Director of the Tadjik Astronomical Observatory (now Institute of Astrophysics of the Academy od Sciences of the Tajikistan, which celebrates its 90-th Anniversary this week). In 1948-1950, he was also Director of the Main Astronomical Observatory of the Ukrainian Academy of Sciences. However, his most long work was as a head of astronomy in the Odessa city, being a director of the Astronomical observatory of the Odessa State (now National) University (ONU) and simultaneously a head of the Department of Astronomy of the Faculty of Physics (1944-1983). Besides, he was, for a partial time, Professor (Department of Higher Mathematics) of the Odessa Institute of Engineers of the Marine Fleet (OIIMF; currently ONMU = Odessa National Maritime University), and, for some time, a Chair of this Department. Also lectured in some other institutes in Odessa. He was involved in numerous state commissions. In 1957 (also an anniversary, 65-th !), there was an International Geophysical Year, preparation for the launch of the first satellite. Two sub-urban observational stations in Mayaki and Kryzhanovka villages were built to this date. The most important achievement was the creation of the "Sky Patrol" 7-camera Astrograph, at which 100 000+ photo negatives had been obtained till 1988. This plate collection, according to the number, is 3-rd in the world after that in the Harvard Observatory (USA) and Sonneberg (Germany). Also, an All-USSR "Bolid net" was organized

together with Prof. E.N. Kramer, as well as the observations of satellites. He hardly contributed to the Public Outreach.

His popular books were very popular: “What and How to Observe in the Sky” (6 editions), “Variable Stars and Observations ofThem), "The Beacons of the Universe", “Variable Stars and their Importance for the Studies of the Universe” and others. Hundreds of people attracted to science (not only astronomers and mathematicians). Only 2 (from 22) scientific monographs were translated into English: "RR Lyr-type stars" (1966) and "Eclipsing variable stars" (1971). He founded he journal “Notes of the Astronomical Observatory”, which, was renamed in 1992 to “Odessa Astronomical Publications” and is edited in English. At the last years of his life, various directions were actively developing in the observatory: eclipsing binary stars (V.G. Karetnikov), pulsating variables (Yu.S.Romanov), stellar spectroscopy (N.S. Komarov), meteorsand comets (E.N.Kramer), satellites (Yu.A. Medvedev), creation of telescopes (L.S. Paulin and N.N. Fashchevsky). The radio-telescope URAN-4 was built also in Mayaki, in a close collaboration with Radio-astronomical Institute of the Ukrainian Academy of Sciences (M.I. Ryabov). The mirror of the 1-m telescope was made in Odessa and was later transferred and installed in the Vihorlat Astronomical Observatory (Slovakia) after his death by Dr. Igor Kudzej and Pavol Dubovský.

The biography and articles on his scientific way in English were publish ed by V.G.Karetnikov, I.L.Andronov. O.E.Mandel, I.B.Vavilova, M.Yu.Volyanska) in memorial articles in “Odessa Astronomical Publications” (ADS codes 1997OAP....10...10K, 2003OAP....16....5A, 2007OAP....20....6V, 2017OAP....30..252A, 2017OAP....30..256V)

Ukrainian cosmonaut Pavlo Popovych – space researcher

L.S. Bashtova

The State Polytechnic Museum named after Boris Paton at Kyiv Polytechnic Institute named after Igor Sikorskyi

This year, our state celebrates the anniversary date - 60 years of the first Ukrainian cosmonaut Pavlo Popovych's flight into space! He is a special and talented person. Pavlo was born on October 5, 1930 in Ukraine, in the small town of Uzyn. After studying at the military aviation school, he received the profession of a fighter pilot. He had good physical, technical and military training. Also, he was a brave and courageous person. Thanks to these qualities, in 1959 he was selected for the first squad of Soviet cosmonauts. At all stages of preparation for a flight into space, he showed high psychological and physical endurance and a high level of knowledge in the study of new technology. The Ukrainian cosmonaut performed an important mission. From August 12 to 15, 1962, Pavlo Popovych made his first space flight on the «Vostok-4» ship. He became the fourth Soviet cosmonaut and the sixth earthling to make an orbital flight in space.

It was the first group raft of «Vostok-3» and «Vostok-4» spaceships in the history of space exploration and the first space flight that lasted several days. Spaceship «Vostok-3» with cosmonaut A. Nikolaev launched from the Baikonur Cosmodrome a day earlier - on August 11, 1962. It was the first time in the history of manned cosmonautics that P.Popovych guided the ship in space using a manual control system. The ships approached and at certain moments were at a distance of 5-6 kilometers from each other. The first experiments were conducted on radio communication between the crews of two ships in space and mutual photography.Video reports of cosmonauts from orbit were made. For the first time, images of cosmonauts were broadcast on the television and the intervision system. For the first time, a Ukrainian song performed by Pavlo Popovych was heard in orbit.The cosmonaut personally investigated the effect of weightlessness on the human body and mental state. The first conclusions were made regarding the need to introduce physical exercises during long-term flights for muscle training. Cosmonauts tested a new air conditioning system. Clean air was constantly produced in the cabin of the spacecraft, atmospheric pressure and humidity were maintained at the required level.

He was being prepared to perform new complex tasks that had to be carried out for the first time in history. In 1965, it was planned to fly together with the woman cosmonaut on the «Voskhod-4» spacecraft. In 1968, he was supposed to be the commander of the «Soyuz-3» ship that was supposed to dock with the «Soyuz-4» spacecraft. In the same year, he was being prepared for a flight on the «Zond-7» ship to the moon.

In 1974 P. Popovych made his second space flight as the commander of the «Soyuz-14» spacecraft and the «Salyut-3» orbital station together with flight engineer Y.Artyukhin. The «Salyut» station was created for a long-term stay in space orbit and was intended to carry out various scientific and technical studies of the Earth, near-Earth space and deep space. Cosmonauts also studied geological and morphological objects of the earth's surface, atmospheric formations and phenomena, physical characteristics of outer space. A significant part of the mission of Pavel Popovych's flight consisted of research commissioned by the military-industrial complex. During the expedition, the cosmonauts performed complex tasks that allowed us to assess the possibilities of accurate observations of the Earth's surface from space.

Today, his life continues in his descendants, in human memory and in his works. The KPI's library keeps a large collection of his autobiographical and technical books.

Forgotten names of employees of the astronomical observatory. Scientific and pedagogical destinies of Putilina N.M., Polyakova T.M.

L.V. Kazantseva[1], L.S. Bashtova[2]

[1]Astronomical Observatory of Taras Shevchenko National University of Kyiv, Kyiv, Ukraine
[2]The State Polytechnic Museum named after Boris Paton at Kyiv Polytechnic Institute named after Igor Sikorskyi

One of the tasks of the Museum of Astronomy is to collect information from various reliable sources for the biographies of its former employees. Their personal data, places of study and work, scientific topics they worked on while working at the Astronomical Observatory, their publications, participation in the public life of the team, interests and hobbies, memories and stories about them, references and references to them in literature — all this creates a more complete image of an individual who can no longer tell

about himself. At the same time, this information complements the general history of the institution itself during the periods when this or that person worked.

The biographies of the two employees are combined in one review, because their destinies are similar in many respects. Both came to Kyiv from Russia, although they had Ukrainian roots, both after their husbands got a job at the Astronomical Observatory. And both of them lived their entire Kyiv life on the territory of its estate, although they did not work at the scientific institution for a long time, because they switched to teaching work, read various courses at higher educational institutions of Kyiv, including Kyiv Polytechnic Institute. Collected archival data, materials of the Museum of Astronomy and documents handed down from relatives allow us to recreate the images of these employees with an interesting fate.

History of the Cosmonautics Museum

H. Ivanova

Department of aviation and Cosmonautics of the Borys Paton State Polytechnic Museum
National Technical University of Ukraine «Igor Sikorsky Kyiv Polytechnic Institute», Kyiv, Ukraine

Cosmonaut is closely connected with astronomy. If a person was not interested in stars and planets, he would never be able to tear himself away from Earth in search of answers to his questions.

The Museum of the history of aviation and Cosmonautics, which was founded in 1989 and became part of the Polytechnic Museum in 2008, tells its visitors not only the participation of KPI in the history of the origin of aviation, but also clearly demonstrates the ways to conquer space. From the creation of the first satellites, to the flight of the first man into outer space. In addition, guests of the museum can get acquainted in detail with the layout of the Moon, recall basic information on astronomy, and even take part in a discussion about whether we are alone in the universe.

This museum is unique, as outstanding veterans of the Baikonur Cosmodrome worked hard to create it, which provided the museum with unique exhibits. For example, Mikhail Yuryevich temper (a participant in military operations in World War II (1941-1945)) presented the museum with a large collection of space badges, envelopes, and books.

General Zavalishin Anatoly Pavlovich, with the assistance of the pilot-cosmonaut of the USSR Titov G. S. , and General Designer of the NPO of Applied Mechanics Mikhail Reshetnev-organized the transfer from the space technology storage base of the «Voskhod» series lander, which was in space in 1965.

The whole story – from the idea to the full functioning - is described in the study.

History of the lunar globe

G. Ivanova[1], L. Kazantseva[2]

[1] Department of aviation and Cosmonautics of the Boris Paton State Polytechnic Museum National Technical University of Ukraine «Igor Sikorsky Kyiv Polytechnic Institute» (Kiev, Ukraine)
[2] Astronomical Museum of the Astronomical Observatory, Taras Shevchenko National University of Kyiv

In two Kiev university museums, visitors ' attention is always attracted by two similar exhibits. The first is a huge globe of the moon with details of the lunar terrain marked on it among the equipment of spacecraft in the DPM NTUU “KPI”. And the second one is medium-sized, but with a part of the sphere that remains unpainted, in the astronomical Museum of AO KNU TS among telescopes and star maps. each one is interesting in its own way, especially when in one year the lunar globe celebrates two “intermediate” anniversaries at once.

60 years ago, the first Globe of the Moon was released with a part of the reverse side of the Earth's satellite depicted on it. It was created on the basis of the first images of the far side of the moon, which were transmitted by the automatic interplanetary station "Luna-3". Then the globe was marked with the first 18 names that were assigned to the relief details of the far side of the Moon.

And 55 years ago, after the probe-3 spacecraft photographed the eastern part of the far side of the Moon at different distances, another Globe was released, on which only 5% of the lunar surface remained unpainted and more than 200 new names appeared in honor of famous scientists.

A brief history of globes, their varieties, collections of ancient Globes in museums around the world, creating maps of the Moon's surface, chronology and technology for obtaining the first images of the far side of

the Moon, features of the structure of the moon's globe, names of Ukrainians on the lunar surface and, of course, the history of these Globes-exhibits of our museums – all this is considered in our study.

Simon Marius (1573-1625) is an independent discoverer of Jupiter's satellites

M. V. Lashko

Main Astronomical Observatory of NAS of Ukraine

In 1614 german astronomer Marius published the results of his observations of Jupiter in a book “Mundus Iovialis anno MDCIX Detectus Ope Perspicilli Belgici ("The Jovian World, discovered in 1609 by means of the Dutch Telescope"), in which he claimed that he had observed Jupiter's satellites before Galilei, in November 1609. But Marius used the Julian calendar, and the dates of his observations corresponds to 8 January on the Gregorian calendar.

The publication of Mundus Iovialis led to a dispute with Galileo, who in 1623 unreasonable accused Marius of plagiarism, and his authority was damaged for many years. But Marius proposed the modern names of the satellites (Io, Europa, Ganymede and Callisto).

At the end of his work, Marius published a table of the positions of the four Jovian satellites for some years in the past and the future, proving that he had early observations separate from those of Galileo. According to his precisive observations of the Galilean satellites he calculated better periods of revolution and orbital elements for them than did Galileo. He also concluded from his observations of the Galilean satellites that they must orbit Jupiter while Jupiter orbits the Sun.

Simon Marius also was one of the first astronomers who observed the Andromeda nebula, with telescope. In 1612 he measured the diameter of the Andromeda nebula and discerned it as having a dull, pale light which increased in brightness toward its center. In 1611 in his almanac Prognosticon Astrologicum he published independent discovery of the phases of Venus

Also he observed the location of Tycho Brahe's supernova of 1572 and found a star.

Marius drew conclusions about the structure of the universe from his observations of the Jovian satellites and the stellar disks. The stellar disks

he observed were caused by diffraction of his telescope, as stars are too distant for their physical disks to be detected telescopically, but Marius interpreted them to be physical disks, like the planetary disks visible through a telescope.

Numismatic collection of Astronomy and Space topics of the Astronomical Museum of Astronomical Observatory of Taras Shevchenko National University of Kyiv

A.M. Mozgova[1], L.V. Kazantseva[1]

[1]Astronomical Observatory of Taras Shevchenko National University of Kyiv, Kyiv, Ukraine

The Astronomical Museum of the Astronomical Observatory of Taras Shevchenko National University of Kyiv has the status of a scientific and technical departmental museum with research and educational functions in accordance with the Regulations and Certificate of Registration. Accordingly, an active work is done on cataloging and study of funds, further researches of selected topics, increasing of collections and saving them, exhibition and popularization. As of 2022, the museum's funds include about 25,000 museum objects, which are divided into thematic and memorial collections. One of the smallest, thematic numismatic collection includes only 24 storage units. It was formed according to the principle of representation of astronomical and space topics. But it also included money signs that convey signs of time for the possibility of using them in memorial exhibitions.

In general, the following thematic blocks can be distinguished in the numismatic collection of AM AO KNUTSh – jubilee and commemorative coins dedicated to individual personalities, anniversaries of scientific institutions, certain scientific events, space exploration, and certain symbolic circulating money. The collection includes coins from several countries – Ukraine, Poland, Bulgaria, the USA, the USSR, and even the Transnistria Governorate. This collection was formed in the 21st century, although the chronological boundaries of the collection are much wider and cover the period 1937–2021. The lower date is due to the oldest item in the collection – «3-kopecks» coin of 1937 that found recently on the Observatory's territory and perhaps it was held in the hands of Professor P.K. Nechyporenko, who was an employee and inhabitant of the

Observatory and who was shot in September of the same year in the cells of the NKVD. The collection also includes coupons from the 1990s of independent Ukraine, a 20 zloty coin dedicated to the flight of the first Polish cosmonaut – Miroslaw Hermaszewski, commemorative coins for the anniversary of Kyiv and Mykolaiv observatories, for the World Year of Astronomy, for the 100th anniversary of Professor S.K. Vsekhsviatsky who was the former director of the Observatory and the head of Astronomy Department of our university and others. An interesting exhibit of bonistics – a paper banknote of 10 Bulgarian levs of 2020 with the image of astronomical instruments. It is dedicated to Petar Beron – a Bulgarian scientist, educator, teacher, representative of the Bulgarian national revival. The banknote was put into circulation by the Bulgarian National Bank in 2020. The materials of the collection items are represented by silver, nickel, nickel silver, copper, copper-nickel alloy. Most of the exhibits are made of nickel silver. The sources of exhibits to the numismatic collection of the Astronomical Museum are donations by employees and visitors.

The numismatic collection of the AM AO KNUTSh is an important scientific source for the study of the history of astronomy and cosmonautics. At the same time, it demonstrates the interest of society in different countries to science and the space industry, the ways to honor the memory of prominent personalities and scientific projects. The filling of the numismatic collection of the AM AO KNUTSh continues and we invite the participants of the conference to join this process.

Museum of magnetic recording technology NDI EMP

O. Provozin

JSC "Research Institute of Electromechanical Devices", Kyiv, Ukraine

Museum of magnetic recording technology, creations by enthusiasts at the Kiev NDI of electro-mechanical devices - if the Head Office of the Territory was created and serial production of magnetic recording equipment and the creation of various kinds of information.

There are no similar museums in Ukraine at all, with the exception of small expositions in the National Mu-seum of Cosmonautics named after S. Korolev in Zhytomyr and in the State Polytechnic Museum of Ukraine at NTUU "KPI" named after I. Sikorskyi. The institute was created to meet the needs of the KGB and Minaviaprom of the USSR, as well as a new

direction branched off from it - cosmonautics, in the equipment for recording and reproducing language information. The need to preserve the operational impressions of cosmonauts, including in emergency situations, led the creators of rocket and space technology to the need to use magnetic recording and speech reproduction equipment on board, and pulse (digital) information intercepted by radio and radio technical intelligence systems for use on board the SHSZ AMZV - in household tape recorders.

From the first years of its existence, the EMP Research Institute was entrusted with the development and supply of equipment in the following space directions by decrees and orders at the highest level in the USSR: equipment for recording and reproducing speech signals on board manned space objects. The famous "Zvezda" tape recorder was created in 1960 as the first swallow for space, thanks to which Yuri Gagarin's voice was preserved, equipment for recording and reproducing information for unmanned objects.

During 1960-1992, the experimental production of the Research Institute of EMP carried out single and small-batch production of tape recorders for manned and unmanned KK and communication satellites. According to the results of its activities, the EMP Research Institute was designated as the leader in the count-ry for the development of special purpose magnetic recording equipment for defense and other purposes, as well as for household magnetic sound and video recording equipment.

The initiator of the creation of the museum of the enterprise was the former deputy director of the EMP Research Institute V. Zvolinsky, who proposed to place it in the meeting hall of the Scientific and Technical Council of the EMP Research Institute and KNPO "Mayak".

Among the main developments of the EMF Research Institute presented in the exposition: peech recording equipment; equipment for recording and reproducing speech equipment for recording and reproducing digital signals; equipment for recording and reproducing voice messages for aircraft - on-board voice recorders, later the so-called "black boxes”; equipment for reproducing voice announcements for aircraft - on-board voice announcers (informants) about emergency situations;equipment for equipping measuring systems in the interests of the "Uzor" series aircraft;information conservation equipment for radio intelligence systems and complexes; equipment for video recording and video reproduction of black and white (for the Su-24 aircraft) and color images – VCR "Krystal" and, respectively, "Kladka-C".

An interesting find is the working weekdays of the TMZ museum

O. Provozin

JSC "Research Institute of Electromechanical Devices", Kyiv, Ukraine

Exhibition of the TMZ Museum in the fall of 2022. replenished with very interesting materials. An employee of the Kyiv branch of the National Center for Aerospace Education of Youth named after A. M. Makarov, V. M. Holovaschuk, addressed me. with a request to repair the special tape recorder "Zvuk-1" (M64), which belonged to the veteran of the Baikonur Cosmodrome Lapidus B.G. (probably it was used at the Baikonur Cosmodrome). The tape recorder, despite the fact that it was produced at p/s 1 in Kyiv back in 1964. managed to restore and bring it to working condition. This was done by Oleksandr Galimov, a 4th-year student of Technical College No. 3 in Lodz (Poland), who at that time was doing an internship at JSC «NDI EMP». He turned out to be a great connoisseur of tape recorders and reel-to-reel ones in particular, as well as an advanced self-taught radio amateur.

We were even more surprised when we put the tape reel that was with it on the tape recorder and turned on the playback mode on the tape recorder. It revealed records of the pre-launch training of the «Soyuz-21» spacecraft with cosmonauts B. Volinov (call sign "Baikal-1") and V. Zholobov (call sign "Baikal-2") on July 4, 1976, their conversations with the flight director and the cosmonaut O. Leonov (call sign "Almaz"), who, as an already experienced cosmonaut, gave them advice and instructions and wishes for the flight. There are also further negotiations between the "Baikal" and the TSUP during the first revolutions of the spacecraft around the Earth.

The "Baikals", as it is already known, had a 49-day flight ahead of them with a rich program to the «Salyut-5» orbital station, which they successfully completed.

For our museum, this is a very significant find, since the EMF Research Institute and cosmonaut-flight engineer V.Zholobov were connected by joint work - after his release from the cosmonaut detachment, V.Zholobov worked for some time as an assistant to the Director of the EMF Research

Institute - the General Director of KNVO "Mayak" V.Antonov and left a good memory for the results of his work.

46 years have passed since the recordings were made, but their quality has proven to be timeless, the voices of the cosmonauts are recognizable. I called Vitaly Mykhailovych (by the way, he is a native of Ukraine - the village of Stara Zbur'ivka, Holopristany District, Kherson Region, he is now 85 years old) and told him about our find, he was happy and said that there is no such record in the family archive. However, we agreed that when we digitize the recording, we will transfer it to him on a flash drive, since tape recorders have not been used in the family for a long time, but there is a laptop.

Therefore, our Museum now also has a very rare and significant recording, which we demonstrate on the "Zvuk-1" 1968 tape recorder we have. release Thus, another interactive exhibition appeared in the TMZ Museum next to the stand for demonstrating the operation of the lunar tape recorder "Malysh-B" and the tape recorder "Pygmey" for the program of the joint flight "Soyuz" - "Apollo" and the musical tape recorder "Arfa-K" for raising the tone of cosmonauts during flights on orbital stations.

History of astronomical observations of military satellites by the station for visual-optical observations of artificial Earth satellites No. 1023

S.A. Salata[1], L.V. Kazantseva[2]

[1]Department for the History of War and Martial Arts of the Research Center of Military History, The National Defense University of Ukraine named after Ivan Cherniakhovskyi
[2] Astronomical Observatory of Taras Shevchenko National University of Kyiv, Kyiv, Ukraine

The first scientific works with the use of military and reconnaissance satellites, officially declassified to date, are reviewed and analyzed. Since most of the developments on this topic were conducted in parallel, the observational results obtained had a double meaning: scientific, which is known to the general public, and military, which is classified.

The Kyiv station for visual-optical observations of artificial Earth satellites (Station No. 1023) was active from 1957 to 1983, but some separate observation programs were irregularly conducted until 1992 as part of the scientific programs of the Kyiv Astronomical Observatory. Over the years, more than 93 thousand target designations were received from the ephemerical center to track more than 400 satellites and 77 thousand positions of artificial celestial objects were determined at specific moments of their passage over Kyiv.

The observation programs included almost all satellites launched at that time, including reconnaissance, navigation, military communications satellites and satellites for the early warning of intercontinental ballistic missiles launching and nuclear tests. All of them were observed under encoded numbers in the general stream. And only recently it became possible to understand the observation of which satellite programs Station No.1023 indirectly participated in. This is, in particular, the WS-117L program within which the satellites were configured to perform various reconnaissance missions, including photo reconnaissance, infrared missile launch warning and electronic reconnaissance. NASA's "Explorer" scientific program, within which, on the one hand, research in atmospheric physics, geophysics, heliophysics and astrophysics from space was performed, and on the other hand, satellite telemetry analysis was conducted for the high-altitude nuclear weapons tests of Operation "Argus".

For the GRAB series of satellites, a scientific task was announced which involve studying the electromagnetic spectrum of the Sun, determining the impact of solar flares on radio communications disruption, and assessing the level of danger of ultraviolet and X-ray radiation for satellites and future astronauts. But, at the same time, the secret purpose of this series of satellites was to identify the location and capabilities of the Soviet air defense radar systems. The CORONA strategic intelligence satellite program of the US, which was established to observe mainly the territory of the "forbidden areas" of the USSR, China, Vietnam and Cuba from space, while the first satellites of this program were made secret and launched as part of the space technology development program called Discoverer. The "Zenit" program of the Soviet military photoreconstruction satellites had the task of obtaining photographs of the Earth's surface with the highest possible resolution and was launched within the general series of "Cosmos" satellites.

Station No. 1023) had the main task of determining the celestial coordinates of the satellite during its passage in the field of view of the station and recording the moments when the satellite is located at the main

points of its path relative to the stars. In addition, special attention was paid to the observation of unknown satellite objects, ephemerides for which were not received from the computing center. Thus, spy satellites and other military satellites were detected, the launches of which were not officially announced.

From astrolyabia to sextant (a brief history of the sextant)

Y. Shevela

Zhytomyr National Agroecological University

Since ancient times, orientation (location) in the open sea has been one of the most important tasks of astronomy. It was not by chance that the first civilizations were located either along large rivers or on the coasts of seas. Water spaces provided our ancestors with food and water, the opportunity to change places of residence, and the discovery of new lands. It took several centuries to solve this difficult problem.

For a long time, ancient sailors, in addition to a compass, navigated using an astrolabe and a clock or chronometer. But such a technique did not have high accuracy - the problem was precisely in determining the longitude.

From the 17th century a fairly common device for orientation was the gradstock. The device consisted of two stationary cross rails and one movable at right angles to the sights. But this device had a big drawback: a large error with a strong duck and poor visibility .

The famous English navigator John Davis replaced the lower part of the movable rail of the hailstone with a sector with an arc of 60°, fixed with the rod, and along the sector there was a movable dioptre that made it possible to sight luminaries at different heights (also allowed to abandon the set of rails). This device was widely distributed under the name Davis quadrant. Unlike the hailstock, it was more convenient and durable to use, but the main disadvantages of the hailstock (duck, fog), although reduced, remained. To get rid of this shortcoming, the English astronomers D. Flemsteed and E. Halley fitted a diopter with a doubly convex lens, and a thin thread was stretched across the diopter, dividing the solar disk in half. Thanks to these innovations, the image of the Sun in the diopter became clearer, and the measurement of angles was much more accurate. In 1667, the astronomer of the Paris Academy of Sciences Ozuti Picard proposed to

attach a sight tube to the Davis quadrant, which greatly increased the accuracy, but did not remove the main problems (duck, fog). There was a great need for new technical solutions. First of all, it was necessary to get rid of the need for a very inconvenient combination of three objects.

In 1699, Isaac Newton proposed a solution to replace this shortcoming. Using the works of R. Hook, where he studied the laws of light reflection, he gave a description of two new instruments. The first of them had one mirror, which reflected the light from the object into the optical tube directed at another object. The second one had two pipes located along the radii of the quadrant directed at the objects and measuring the angle between us. Newton did not publish his project (it was published in 1742), but instead offered to announce a competition for the best solution to the "longitude problem", for which the "Longitude Commission" was created in Great Britain, with a large financial reward!

The first option was proposed in 1731 by an English mechanic and astronomer, vice-president of the Royal Society of London, John Hadley. He removed the small sector in the Davis quadrant, and replaced the central diopter with a mirror. The mirror made it possible to visualize two objects located in different directions at the same time.

In 1757, the captain of the English fleet, John Campbell, proposed to increase the sector from 45° to 60°, so that it would be possible to measure angles up to 120°, which was done by John Byrd. Sextants also had various options to solve other inconveniences or shortcomings: e.g. the same J. Hadley attached a water spirit level to the sextant, for use when the sky is not visible.

But to this day, the "classic" version of the sextant by J. Campbell and J. Byrd is used from the mechanical options.

Наукове видання

Астрономія та фізика космосу в Київському університеті

Міжнародна конференція

м. Київ, 18 жовтня – 21 жовтня 2022 р.

Збірка тез доповідей

Підписано до друку 10.05.11. Формат 60x84$^{1/16}$.
Гарнітура Times. Папір офсетний.
Друк офсетний. Наклад 100. Ум. друк. арк. 7,0. Зам. № ККК-НННН.

Надруковано у Видавничо-поліграфічному центрі „Київський університет”
01601, Київ, б-р Т.Шевченка, 14, ☎ 239 3128
Свідоцтво внесено до державного реєстру ДК № 1103 від 31.10.02